GPM Available Products

[As of September 4, 2024.]

Standard Products

Processing Level	Satellite / Instrument / Algorithm	Product [Product Identifier/ Algorithm Key*1]	Key Parameters	File coverage	Available Latest Product Version (Caveats)
1	GPM/DPR/Ku	KuPR L1B [DUB]	Received Power	GPM orbit (Gorbit*)	Ver. 07 (See: page 11~)
	GPM/DPR/Ka	KaPR L1B [DAB]	Received Power	Gorbit	Ver. 07 (See: page 11~)
	GPM/GMI	GMI L1B [G1B]	Brightness Temperature (Tb)	Gorbit	Ver. 07 (See: page 4)
	GPM/GMI	GMI L1C [G1C]	Brightness Temperature (Tb)	1 orbit	Ver. 07 (See: page 5)
	Constellation/ MWS	Constellation L1C [*2]	Inter-calibrated Brightness Temperature (Tb)	Gorbit	Ver. 07 (See: page 5)
2	GPM/DPR	KuPR L2 [DU2]	Reflectivities, 3D Precipitation	Gorbit	Ver. 07 (See: page 25~)
		KaPR L2 [DA2]	Reflectivities, 3D Precipitation	Gorbit	Ver. 07 (See: page 25~)
		DPR L2 [DD2]	Dual Frequency Retrievals, 3D precipitation	Gorbit	Ver. 07 (See: page 25~)
		SLH-DPR L2 [SLP]	Spectral latent heating	Gorbit	Ver. 07 (See: page 39~)
	GPM/GMI/GPROF	GMI L2 [GL2]	Precipitation, Total Precipitable Water	Gorbit	Ver. 07 (See: page 7~)
	GPM/DPR-GMI /COMB	DPR-GMI Comb L2 [CL2]	DPR-GMI retrieval. 3D Precipitation	Gorbit	Ver. 07 (See: page 50~)
3	GPM/DPR	DPR L3 Daily (TEXT) [D3D]	Precipitation	0.1°x 0.1° Daily	Ver. 07 (See: page 25~)
		DPR L3 Daily(HDF5) [D3Q]	Precipitation	0.25° x 0.25° Daily	Ver. 07 (See: page 25~)
		DPR L3 Monthly [D3M]	Precipitation	0.25° x 0.25° Monthly	Ver. 07 (See: page 25~)
		SLH-DPR L3 Gridded orbit [SLG]	Spectral latent heating	0.5°x 0.5° Gorbit	Ver. 07 (See: page 39~)
		SLH-DPR L3 Monthly [SLM]	Spectral latent heating	0.5°x 0.5° Monthly	Ver. 07 (See: page 39~)
	GPM/GMI/GPROF	GMI L3 Monthly [GL3]	Precipitation	0.25° x 0.25° Monthly	Ver. 07 (See: page 10~)
	GPM/DPR-GMI /COMB	DPR-GMI Comb L3 [CL3]	Precipitation	0.25° x 0.25° Monthly	Ver. 07 (See: page 50~)
		DPR-GMI CSH L3 [CSG]	Gridded Orbital Convective Stratiform Heating	0.25° x 0.25° Gorbit	Ver. 07 (See: page 57～)
		DPR-GMI CSH L3 [CSM]	Monthly Convective Stratiform Heating	0.25° x 0.25° Monthly	Ver. 07 (See: page 57～)
	Multi/Multi/GSMaP	GSMaP Hourly (TEXT) [MCT]	Precipitation *3	0.1°x 0.1° Hourly	Ver. 05 (See: page 44~) Ver. 04 (See: page 47~)
		GSMaP Hourly (HDF5) [MCH]	Precipitation *3	0.1°x 0.1° Hourly	Ver. 05 (See: page 44~) Ver. 04 (See: page 47~)
		GSMaP Monthly [MCM]	Precipitation *3	0.1°x 0.1° Monthly	Ver. 05 (See: page 44~) Ver. 04 (See: page 47~)

* Gorbit is the GPM orbit calculated from the southern most point back to the southern most point

GPM Available Products

[As of September 4, 2024.]

Near Real-Time Products

(Near real-time data can be downloaded using SFTP after G-Portal user registration and public key authentication. SFTP directory tree is shown in page 3. *4)

Processing Level	Satellite / Instrument / Algorithm	Product [Product Identifier/ Algorithm Key*1]	Key Parameters	File coverage	Available Product Version
1R	GPM/DPR/Ku	KuPR L1B [DUB]	Received Power	30 min	Ver. 07 (See: page 11~)
	GPM/DPR/Ka	KaPR L1B [DAB]	Received Power	30 min	Ver. 07 (See: page 11~)
	GPM/GMI	GMI L1B [G1B]	Brightness Temperature (Tb)	5 min	Ver. 07 (See: page 4)
	GPM/GMI	GMI L1C [G1C]	Brightness Temperature (Tb)	5 min	Ver. 07 (See: page 5)
2R	GPM/DPR	KuPR L2 [DU2]	Reflectivities, 3D Precipitation	30 min	Ver. 07 (See: page 25~)
		KaPR L2 [DA2]	Reflectivities, 3D Precipitation	30 min	Ver. 07 (See: page 25~)
		DPR L2 [DD2]	Dual Frequency Retrievals, 3D precipitation	30 min	Ver. 07 (See: page 25~)
	GPM/GMI/GPROF	GMI L2 [GL2]	Precipitation, Total Precipitable Water	5 min	Ver. 07 (See: page 7~)
	GPM/DPR-GMI /COMB	DPR-GMI Comb L2 [CL2]	DPR-GMI retrieval. 3D Precipitation	30 min	Ver. 07 (See: page 50~)
3R	Multi/Multi/GSMaP	GSMaP Hourly (HDF5) [MFW]	Precipitation *3	0.1°x 0.1° Hourly	Ver. 05 (See: page 44~) Ver. 04 (See: page 47~)
		GSMaP Hourly (TEXT) [MFT]	Precipitation *3	0.1°x 0.1° Hourly	Ver. 05 (See: page 44~) Ver. 04 (See: page 47~)

Auxiliary Products

Processing Level	Satellite / Instrument / Algorithm	Product [Product Identifier/ Algorithm Key*1]	Key Parameters	File coverage	Available Latest Product Version
AUX.	Auxiliary Data (JMA/GANAL)	Environmental data extracted KuPR swath [DU2/ENV]	Temperature, Air Pressure, Cloud Water Vapor, Liquid Water	Gorbit	Ver. 07
		Environmental data extracted KaPR swath [DA2/ENV]	Temperature, Air Pressure, Cloud Water Vapor, Liquid Water	Gorbit	Ver. 07
		Environmental data extracted DPR swath [DD2/ENV]	Temperature, Air Pressure, Cloud Water Vapor, Liquid Water	Gorbit	Ver. 07

GPM Available Products

[As of September 4, 2024.]

Notes

*1 File Naming Convention

GPM product file naming conventions is as below, and algorithm key is corresponding to (7).

GPMxxx _ sss _ YYMMDDhhmm _ hhmm _ nnnnnn _ LLS _ aaa _ VVv . h5

(1)Mission ID
(2) Sensor ID
(3) Scene Start
(4) Scene End
(5) Orbit Number
skip for NRT data
(6) Process Level
(7)Algorithm Key
*indicated in product list and below note (*2) for L1C*
(8)Product Version

start and end time for L3 product
hourly file: YYMMDDhhmm_H
daily file: YYMMDD_D
monthly file: YYMM_M

*2 Product Identifier for Constellation L1C

Satellite	Instrument	Product Identifier / Algorithm Key
TRMM	TMI	TMI

*3 Introduced satellite/instrument data in GSMaP

Term	Satellite / Instrument
2014.3.1~2014.3.4	TRMM/TMI DMSP-F16/SSMIS DMSP-F17/SSMIS DMSP-F18/SSMIS GCOM-W/AMSR2 METOP-A/AMSU-A, MHS METOP-B/AMSU-A, MHS NOAA-18/AMSU-A, MHS NOAA-19/AMSU-A, MHS
2014.3.4~	GPM/GMI (No data during Oct.22-24,2014) TRMM/TMI (No data from Apr.8,2015 onward) DMSP-F16/SSMIS DMSP-F17/SSMIS (No data from May 1,2018 onward) DMSP-F18/SSMIS DMSP-F19/SSMIS (No data from Feb.11,2016 onward) GCOM-W/AMSR2 METOP-A/AMSU-A, MHS * (No MHS data from Mar.27 to May 20, 2014) METOP-B/AMSU-A, MHS NOAA-18/AMSU-A, MHS (No data from Dec.24,2018 onward) NOAA-19/AMSU-A, MHS
2021.12.1~	See: https://sharaku.eorc.jaxa.jp/GSMaP/guide.html#05

*4 G-Portal SFTP directory tree

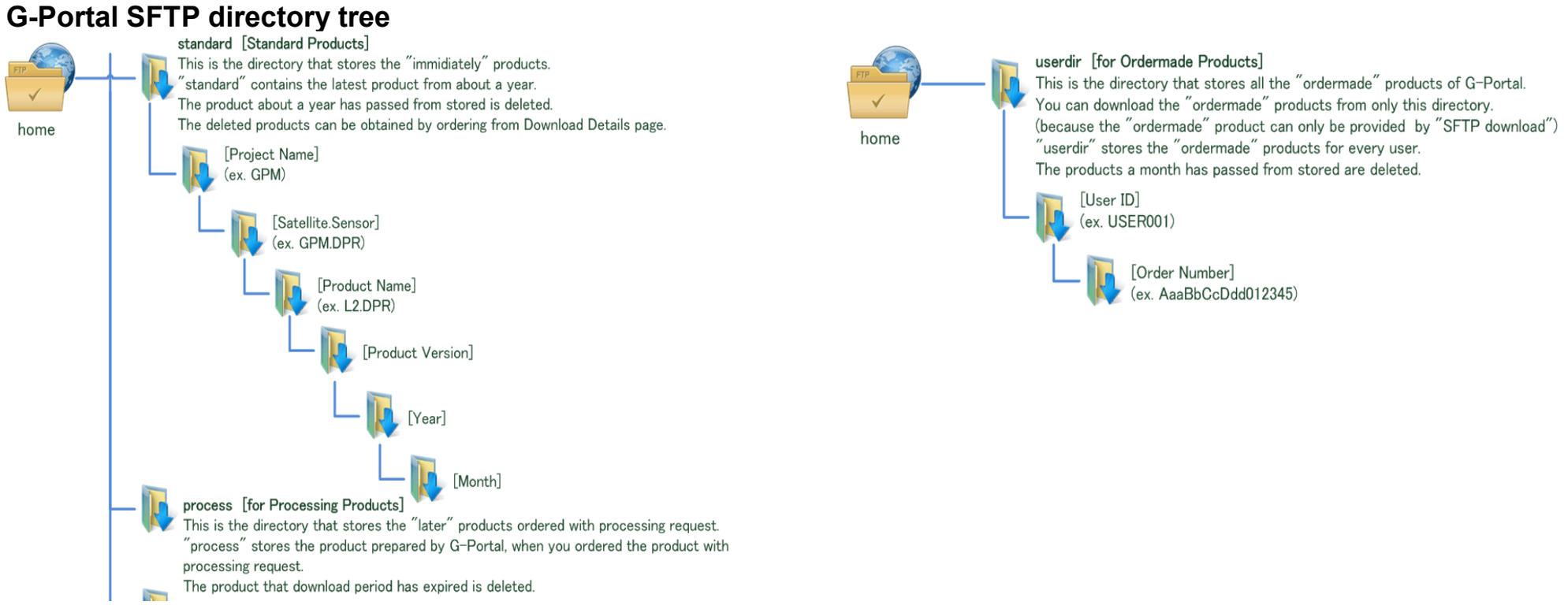

RELEASE NOTES OF GPM VERSION 07 GMI/TMI 1B/BASE

The PPS V07 GMI 1B/BASE have no calibration changes from V05 GMI 1B/BASE. However, a module is implemented to perform calibrations under conditions of missing all cold counts or all hot counts by utilizing the noise diode counts.

The PPS V07 TMI 1B/BASE applied a new Tb correction developed by UCF based on main reflector physical temperatures. The maximum Tb change is around 0.5K.

$$T_{b_i} = \frac{T_{apcv8_i} - T_{phy_i} * \varepsilon_i}{1 - \varepsilon_i} \qquad (2)$$

Reflector Physical Temperatures, Tphy, is functions of solar-beta-ang & orbit-phase.
Final Tphy Tables:

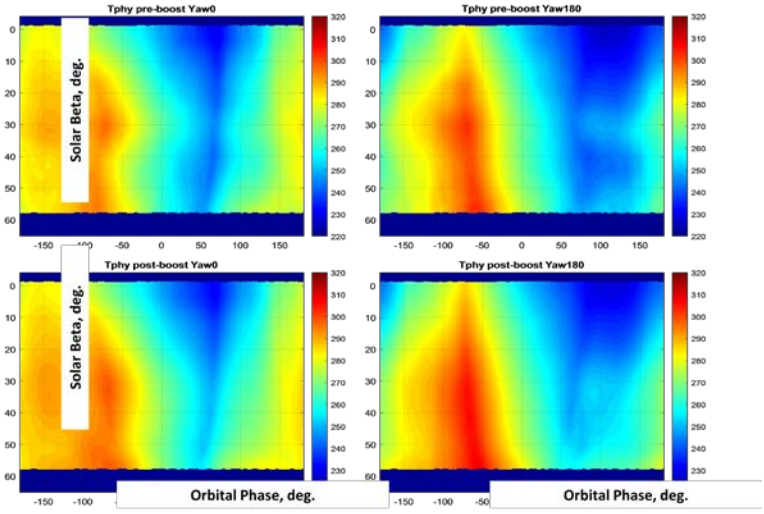

- Rows = Solar beta angle in deg. [-4 to 65 deg.(yaw0) and 4 to -65 deg.(yaw180) in 0.25 deg. step] > 277 rows
- Columns = Phase from orbit midnight in deg. [-180 to 180 deg. in 1 deg. step] > 361 columns
- For yaw=180, beta was reversed (i.e., beta=-1*beta;)

Level 1C Version 07 (V07) Release Notes

This Level 1C Version 07 (V07) release involves the following changes from the previous release in the GPM radiometer constellation.

1. A new parameter, “sunLocalTime” (local solar time), was added to all GPM V07 Level 1C products.

2. Level 1C V07 GMI brightness temperature (Tc) remains unchanged from V05. There is no GMI calibration update. A minor update was implemented to handle long-term failure of cold load and/or hot load.

3. Level 1C V07 TMI intercalibrated brightness temperature (Tc) differs from V05 by as much as 0.7 K due to the following updates:
   a. Updated emissive reflector correction in L1B/1Base. V07 corrects a minor error discovered in the V05 emissive reflector correction and improves the simulated brightness temperatures used in the correction algorithm with ERA5 inputs instead of GDAS.
   b. Adjusted first pixel time in L1B/1Base. This changes the geolocation by about 0.95 kilometers forward along-track for the 10 GHz channels and 0.15 km back along-track for the 19-85 GHz channels.
   c. Updated intercalibration adjustments (XCAL2021-V) to account for the brightness temperature changes. Table adjustments range from 0.1 to 0.2 K depending on channel.

Acronym List

Below are the acronyms and abbreviations used in this document.

AMSR2	Advanced Microwave Scanning Radiometer 2
AMSRE	Advanced Microwave Scanning Radiometer Earth Observing System
AMSUB	Advanced Microwave Sounding Unit – B
ATMS	Advanced Technology Microwave Sounder
ECMWF	European Centre for Medium-Range Weather Forecasts
GCOM-W1	Global Change Observation Mission – Water
ERA5	ECMWF Reanalysis V5
GDAS	Global Data Assimilation System
GMI	GPM Microwave Imager
GPM	Global Precipitation Measurement
L1B	Level 1B
METOP-A	Meteorological Operational Satellite – A
MHS	Microwave Humidity Sounder
MSPPS	Microwave Surface and Precipitation Products System
NOAA	National Oceanic and Atmospheric Administration
NPP	National Polar-Orbiting Partnership
ORB	Orbital
SAPHIR	Sondeur Atmospherique du Profil d'Humidite Intertropicale par Radiometrie
SDR	Sensor Data Record
SSMI	Special Sensor Microwave Imager
SSMIS	Special Sensor Microwave Imager/Sounder
Tb	Brightness Temperature
Tc	Intercalibrated Brightness Temperature
TIROS	Television Infrared Observation Satellites
TMI	TRMM Microwave Imager
TOVS	TIROS Operational Vertical Sounder
TRMM	Tropical Rainfall Measuring Mission
V05, V07	Version 5, Version 07
V1, V2	Version 1, Version 2
X-CAL	GPM Intercalibration Working Group

May 3, 2022
ATBD GPM V7: http://rain.atmos.colostate.edu/ATBD/ATBD_GPM_V7_May15_2021.pdf

Release Notes for GPROF V7 Public Release

The Goddard Profiling Algorithm is a Bayesian approach that nominally uses the GPM Combined algorithm to create its a-priori databases. Given the importance of these databases to the final product, they are worth reviewing before discussing particular changes to the algorithm. GPROF V03 was implemented at the launch of the GPM mission and thus had no databases from the GPM satellite itself. Instead, databases were made from a combination of TRMM, Cloudsat, ground based radars and models. V04 used the GPM generated databases but had a very short lead time as the radar and combined algorithm were in flux until nearly the date of the public release. Because the V04 of the Combined algorithm appeared to significantly overestimate precipitation over land, the a-priori databases were constructed from the Combined Algorithm (V04) over ocean, but the DPR Ku (V04) over land and coastal regions. The very short lead time to produce the a-priori databases led to insufficient testing of GPROF V04 that resulted in some less-than ideal retrievals.

GPROF V05 retained the previous version (i.e. V04) of the Combined and DPR-Ku products for its databases, but improved some of the ice hydrometeor simulations in order to get better agreement between computed and simulated brightness temperatures. Additional changes were made to retrievals of high latitude oceanic drizzle and snowfall over land as the DPR sensitivity of 12 dBZ (and therefore the Combined and Radar products) was shown to miss substantial amounts of drizzle and light to moderate snowfall events. Drizzle in the a-priori database was matched to the CloudSat based probability of rainfall and this was partitioned between cloud- and rain water. This increased rain water at high altitudes to agree better with CloudSat and ERA and MERRA re-analyses, but continued to be low relative to these estimates.

There is not GPROF V06. Instead, GPROF jumped to GPROF V07 to mirror the other GPM products that were produced starting in May 2022. In GPROF V07, the a-priori databases were constructed singularly from the Combined Radar/Radiometer Algorithm (V07) where it sees precipitation, while non-precipitating and light drizzle (up to 0.2 mm/hr) are created from the operations Microwave Integrated Retrieval System (MiRS) Optimal Estimation retrieval. The GPROF V07 database, as done previously, uses only the middle 21 pixels of the radar scan. This subset of the CMB product produces more rain than the entire swath, and V7 produces substantially more rain than the CMB product used in GPROF V05. Rain rates have thus increased significantly, in the 12% range globally.

Some changes were made to the coast and land surface types for GPROF V07. Previous versions of GPROF showed spurious precipitation in coastal areas. To improve estimates, the V05 coast surface class was split into three classes of decreasing ocean/water percentages: water coast, mixed coast and land coast.

Similarly, areas of complex terrain have been identified as lacking orographically enhanced precipitation, compared to ERA5 and High Resolution Rapid Refresh (HRRR) model data. A mountain rain and mountain snow class are included in GPROF V07. For the mountain rain class, the surface type was further subclassified with an airmass lifting index (ALI), based on whether atmospheric conditions were stratiform and orographically enhanced. The Combined product precipitation used int eh a-priori database for the two new mountain classes was also scaled to match ERA5, which was considered to be a better mountain precipitation climatology.

Over land, the US based MRMS data was used to build a-priori databases for snow covered surfaces of each of the constellation's radiometers. Five years of MRMS data were matched up with individual satellite overpasses, compared to two years in GPROF V05. While MRMS data removed much of the low bias that GPROF V04 had over snow covered surfaces, further adjustments were made to make the MRMS data spatially consistent with SNOw Data Assimilation System (SNODAS) precipitation estimates.

Sea ice a-priori databases in GPROF V07 are created with ERA5 precipitation, since the DPR is insufficient over these surface types. As with the MRMS data, the sea ice database was only 2D and did not contain the vertical hydrometeor profiles, so no profile information is available from the GPROF retrieval over sea ice covered surfaces.

A change has been made to the GPROF V05 profile species, which were: rain water content, cloud water content, ice water content, snow water content and graupel/hail content. In GPROF V07, the profile species are: rain water content, cloud water content, snow water content, graupel/hail content and latent heating. However, the graupel/hail content and latent heating profiles are currently set to missing, with the latter to be implemented in the next version.

A final modification made to GPROF is the determination of a precipitation threshold. GPROF V04 reported an unconditional rain rate and a probability of precipitation, it was up to the user to set a threshold (either in probability or rain rate) if rain/no rain information was needed. While GPROF V05 reported the same information, the algorithm internally decided if the pixel was precipitating or not, and non-precipitating pixels were set to zero rainfall. This required the algorithm to replace the missing rain by slightly increasing the precipitation in the pixels that were deemed raining. GPROF V07 reverts back to the unconditional rain rate and probability of precipitation being reported, as it is really not possible for passive microwaves to distinguish clouds from very light rain in an unambiguous manner. To accommodate users who need a binary yes/no answer, a new precipitation flag has been added to the output. If the algorithm determined the pixel was most likely precipitating, the 'precipitationYesNoFlag' is set to raining.

Limited validation of GPROF V07 for GMI shows better correlations and smaller biases than GPROF V05. Statistics were run over the Continental United States with MRMS data and globally with Combined data. Even more limited validation has been done on snow due to the difficulty in getting reliable ground-based measurements.

GPROF V07 chose to wait for the latest interation of the GPM CMB product in order better to synchronize the products. The short lead time to produce the a-priori databases, unfortunately, also led to less than full testing of GPROF V07. Little validation has been done on the constellation radiometers beyond limited comparisons with GMI (or TMI for earlier sensors) to ensure that the retrieval is performing as expected.

The GPROF V07 output file 'airmassLiftIndex' has replaced the V05 parameter labeled 'CAPE' (set to missing in GPROF V05), as it is not used.

Sims, E.M. and G. Liu, 2015: A Parameterization of the Probability of Snow–Rain Transition. *J. Hydrometeor.,* **16**, 1466–1477, doi: 10.1175/JHM-D-14-0211.1.

National Operational Hydrologic Remote Sensing Center. 2004. *Snow Data Assimilation System (SNODAS) Data Products at NSIDC, Version 1*. Boulder, Colorado USA. NSIDC: National Snow and Ice Data Center. doi: https://doi.org/10.7265/N5TB14TC.

GPM Level 3 GPROF Version 07 Information

Version 07 Release Notes:

This Level 3 GPROF Version 07 release involves the following changes from the previous (Version 05) release:

1. Product format change:
   Added dimension variables such as lat, lon, layer, lat_bnds, lon_bnds, layer_bnds. Removed cloudIce variable but added graupel and latentHeating variables.

2. Total number of precipitation pixels (npixPrecipitation):
   In Version 05, pixels with pixelStatus=0 and surfacePrecipitation > 0 are counted as precipitation pixels. In Version 07, pixels with pixelStatus=0, surfacePrecipitation > 0 and precipitationYesNoFlag=1 are counted as precipitation pixels.

Description:

The L3GPROF algorithm provides monthly and daily mean precipitation and related retrieved parameters from the Level 2 GPROF precipitation profiling algorithm for the GPM core and constellation satellites.

Each L3GPROF product contains global 0.25^{o} x 0.25^{o} gridded monthly/daily unconditional means and pixel counts. Monthly product filenames start with 3A-MO or 3A-CLIM-MO, and daily product filenames start with 3A-DAY or 3A-CLIM-DAY.

For example:
3A-MO.GPM.GMI.GRID2021R1.20161201-S000000-E235959.12.V07A.HDF5
3A-DAY.GPM.GMI.GRID2021R1.20161201-S000000-E235959.336.V07A.HDF5
3A-CLIM-MO.GPM.GMI.GRID2021R1.20161201-S000000-E235959.12.V07A.HDF5
3A-CLIM-DAY.GPM.GMI.GRID2021R1.20161201-S000000-E235959.336.V07A.HDF5

Current available L3GPROF V07 products are listed in the following table:

Product ID	Radiometer	Satellite
3GPROF	AMSR2	GCOM-W1
3GPROF	ATMS	NPP NOAA20
3GPROF	GMI	GPM
3GPROF	MHS	NOAA-18 NOAA-19 METOP-A METOP-B METOP-C
3GPROF	SSMI/S	F16 F17 F18 F19

Release Notes for the DPR Level 1 products

All users of DPR Level 1 data should keep in mind the following changes in Version 07B products.

＜Minor changes in the DPR Level 1 products from Version 07A to Version 07B＞

The GPM Core Observatory satellite performed orbit boost maneuvers on Nov. 7 and 8, 2023 that raised its altitude from 407km to 442km. Details show at the following link.

https://gpm.nasa.gov/missions/gpm/orbit-boost

The orbits in which this operation was performed are shown operation status in the following link.

https://gportal.jaxa.jp/gpr/information/product

1. Changes of the sensitivity, the spatial resolution and the swath width
   The sensitivity, the spatial resolution and the swath width in the DPR instrument were changed. See full descriptions by the following link.
   https://www.eorc.jaxa.jp/GPM/en/boost.html

2. Update the VPRF table.
   A new VPRF (Variable Pulse Repetition Frequency) table for the post-boost was installed in the KuPR and the KaPR. Corresponding VPRF table was implemented in the DPR Level 1 algorithm as well.

3. Update altitude information.
   The DPR Level 1 product stores two altitude information that are `dprAlt` and `scAlt`. After the orbit boost, the altitude for DPR operation was stored in the `dprAlt` and real spacecraft altitude was stored in the `scAlt`. See full descriptions by the following link.
   https://www.eorc.jaxa.jp/GPM/doc/algorithm/GPM_Orbit-boost_DPR-note_20240304A.pdf

4. Update the timing delay.

The observation timings in the along-track direction of the KuPR and the KaPR were changed to adjust the beam matching of those footprints for the orbit boost.

＜Major changes in the DPR Level 1 products from Version 05C to Version 07A＞

1. Refinement of the scan angle table (KuPR)
   JAXA implements a small adjustment (about 0.024 deg) of the scan angle table used in the geolocation calculations based on a statistical analysis of KuPR's geolocation. Note that KuPR's hardware setting related to beam pointing does not change, and a parameter in the scan angle table for calculating the geolocation of beam is updated.
2. A new quality flag for mirror image (KuPR and KaPR)
   `binMirrorImage` which notifies an unusual precipitation at high altitude by the mirror image of DPR is introduced.
3. Swath name change (KuPR)
   A swath name in KuPR Level 1 product is changed from 'NS' to 'FS'.
4. Refinement of a table for gain of phase shifter (KaPR)
   JAXA implements a small adjustment to a table for the gain of phase shifter which is one of the components in the receiver system and is responsible for the DPR's beam direction. This is expected to mitigate an angle bin dependency of the gain depending on the phase shifter setting after the change of KaPR's scan pattern on 21 May 2018. This adjustment results in a maximum change of about 0.5 dB in the received power and noise power of KaPR.
5. New variables related to geolocation (KuPR and KaPR)
   New variables related to geolocation are newly added. They are `sunLocalTime`, `scHeadingGround`, `scHeadingOrbital`, `sunData group`. See full descriptions by the following link.
   https://www.eorc.jaxa.jp/GPM/en/archives.html
6. Update correction values for `startBinRange` (KuPR and KaPR)
   Correction values for the observation start distance is updated. This changes the estimated observation start distance by 16 m for KuPR, 5 m for KaMS, and 56 m for KaHS.
7. Variable definition changed. (KuPR and KaPR)
   The definition of `noiseSampleNumber` is changed to store the actual number of samples measured by the instrument considering the number of independent sample.

＜Minor changes in the DPR Level 1 products from Version 05B to Version 05C＞

JAXA and NASA implemented a small adjustment of the instrument alignments used in the geolocation calculations based on the beam matching adjustments in Version 05B. These shifts in pointing will occur in the V05A/B data once that data is reprocessed as well.

1. The KaPR roll alignment was adjusted so that the calculated beam locations on the surface better match those for KuPR in the cross-track direction. The adjustment changes the KaPR locations by about 100 meters cross track.

2. The KuPR pitch alignment was adjusted so that the calculated beam locations on the surface better match those for KaPR in the along-track direction. The adjustment changes the KuPR locations by about 40 meters along track.

＜Minor changes in the DPR Level 1 products from Version 05A to Version 05B＞

JAXA and NASA implemented a change of the scan pattern of the KaPR on 21 May 2018.

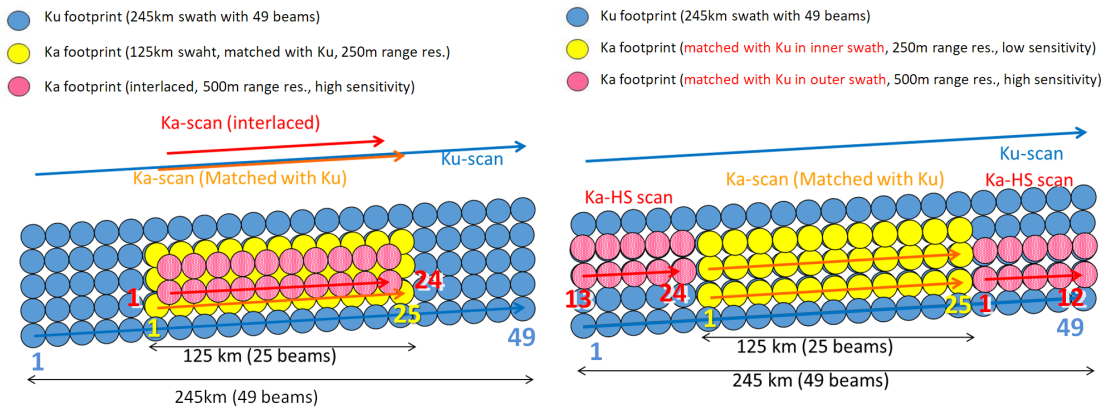

Figure 1. DPR's scan pattern before May 21 2018 (left) and after May 21 2018 (right). KaHS beams scan in the inner swath before May 21 2018, but now they scan in the outer swath and match with KuPR's beams. Numbers in color indicate angle bin numbers for KuPR (blue), KaMS (yellow), and KaHS (red).

According to this event, the DPR Level 1 product version has changed from 05A to 05B. Major effects were summarized as follows.

1. Change of the scan pattern of the KaPR.
   JAXA changed the scan pattern of the KaPR on 21 May 2018. As shown in Fig.1, the high sensitivity beams of KaPR, which is called KaHS, scanned in the inner swath and interlaced between the matched beams of KaPR, which is called KaMS, from the beginning of the mission until May 21. As of May 21, KaHS beams are moved to the outer swath and match with the KuPR beams there so that the dual-frequency algorithm can be applied over the full swath. The format of the product does not change in V05B. The first 12 elements in each of KaHS's scan data that consist of 24 angle bins correspond to the last 12 angle bins of the KuPR angle bins, and the remaining 12 elements correspond to the first 12 angle bins of the following KuPR scan. A warning flag is set in the variable called "dataQuality".

2. Improvement of beam matching between the KuPR and the KaPR.
   JAXA has adjusted the beam directions of the KuPR and the KaPR in order to improve the beam matching between the KuPR scans and KaPR scans. The offset between the KuPR and KaMS footprint centers at nadir has reduced approximately from 300m to 30m since the adjustment on 21 May 2018,.

＜Major changes in the DPR Level 1 products from Version 4 to Version 5＞

1. Changes of the DPR's calibration parameters.
   JAXA improved the DPR's calibration parameters in the Version 5 products based on the new calibration results on orbit. With the new parameters, the measured radar reflectivity factors increase by about +1.3 dB for the KuPR and by about +1.2 dB for the KaPR from the corresponding Version 4 data.

2. Changes of FCIF-LUT.
   The temperature dependence of the FCIF input/output characteristic was improved based on the re-examination of calibration data. The re-examination revealed that the version 4 algorithm compensate the temperature changes too much. In V5, the gain adjustment due to the temperature change is nullified because the actual temperature of FCIF is very stable on orbit.
   The FCIF-LUT for the KuPR near the saturation was improved so that the effect of saturation near the saturation level was mitigated. As for the KaPR,

the modification was not made because saturations do not occur in the KaPR in a normal condition.

3. Data format change
   The following two new variables were added and one variable was modified.
   - 'receivedPulseWidth' that indicates the received pulse width after passing through the band-pass-filter was added.
   - 'totalCoefVersion' that indicates the total version, which consists of the version number of the calibration coefficients and the version number of the FCIF-LUT, was added.
   - 'transReceiverCoefVersion' that indicates the version number of the calibration coefficients was modified.
4. Improvement in noise power calculation
   The definition of the DPR's noise power was changed. Since the effect of the band-pass filter to noise is different from that of the radar echoes (the former has a continuous flat spectrum while the latter has a non-flat spectrum defined by the transmitting pulse shape), the version 4 algorithm used a formula to calculate the noise power that differs from the formula to calculate the echo power. In version 5, the noise power is also calculated with the formula that is used to calculate the echo powers so that the noise power in V5 is the effective noise power that can be compared with echo powers directly.

＜Caveats for the DPR Level 1 products＞

1. Status of the DPR A-side operation

   JAXA changed that the status of the DPR data obtained during the A-side operation in products Version5 (B-side is used in the current standard operation). The reasons for such handling are that the calibration parameters of the DPR A-side are not reliable, because no external calibration of the DPR A-side was carried out on orbit, and the ground test values of the DPR A-side before launch are not reliable either. Therefore, the corresponding scans were attached with identification flags in the DPR Level 1 products, and these scans were treated as missing scans in the DPR Level 2 products. The following table shows the periods of the DPR A-side nominal operation.

Operational mode	Period	Orbit number
SCDP-B/FCIF-A	2014/3/10~3/12, 5/25	171 - 205, 1351-1355
SCDP-A/FCIF-A	2014/3/14~16	232-262
SCDP-A/FCIF-B	2014/3/16~18	263-295

   B-side (SCDP-B/FCIF-B) is used in the rest of the period.

2. Calculation of the DPR's noise power

   The DPR has a special mode to measure background noise in which the average noise power is measured while the transmitter is turned off at each angle bin in the ordinary observation mode ('Noise-A'). This noise power is subtracted from the received power measured at each range bin to extract radar echo power profile. To calculate the echo profile, the effect of the band-pass filter assumes that the echo has the same power spectrum defined by the transmitted pulse shape. Since the received power is the sum of echo power and noise power, the noise power recorded in each profile is the effective noise ('Noise-B') that affect the echoes. In version 4, Noise-A was calculated by assuming that the noise has a flat spectrum. The difference in the conversion formulas to calculate Noise-A and Noise-B created some confusions to the users although the noise was properly subtracted in the products. In order to avoid the confusion, Noise-A is calculated with the same formula that is used to calculate the echo profile (and hence Noise-B) in version 5. (As a result, the noise power calculated by using the hardware design document is the lower than the power stored in the DPR

L1 product. The magnitudes of difference are -2.11dB, -2.41dB and -2.13dB for the KuPR, the KaPR(MS) and the KaPR(HS), respectively.)

3. Beam directions of the KaPR

JAXA uploaded a proper set of phase code to the KaPR on August 6th, 2014. Until that time from April 8th, 2014, the beam pointing directions of the KaPR had small biases. The code error caused a beam match between the KuPR and the KaPR(MS) and affected the KaPR's total antenna gain slightly. After the proper code was uploaded, the beam scans in the proper directions and the bias error were resolved. The DPR Level 1 algorithm was modified to compensate this bias for the antenna gain in this period so that the antenna gain in the products is correct.

4. Reversal of DPR's scan direction

The beam scan direction of DPR had been reversed from the proper direction until JAXA uploaded a proper set of phase code to the DPR at 13:20 UTC on March 18th, 2014. After the proper code was uploaded, the beam has been scanned in the proper direction, i.e., from left to right with respect to the +X forward direction of the satellite.

The DPR Level 1 algorithm was modified to accommodate this change so that the geolocations in the products are correct from the beginning of the mission.

5. Special operations of DPR

The following caveats describe special operations of DPR. You can use these data with your discretion. You can also refer to the DPR invalid data lists at the following web site. https://gportal.jaxa.jp/gpr/information/product

5.1. Operation with the DPR transmitters off

JAXA carried out the receiving only mode to check the DPR receiver system. The orbits in which this operation was performed are shown Appendix-A and operation status in the following site.

https://gportal.jaxa.jp/gpr/information/product

5.2. Change of the DPR receiver attenuator (RX ATT) setting

JAXA has checked the dynamic range of the radar system by changing the attenuator setting in the DPR receivers. The received power in the DPR Level 1

products is not affected, because the offset caused by the receiver attenuator is accounted for in the DPR Level 1 algorithm. The orbits in which this operation was performed are shown Appendix-A and operation status in the following site. https://gportal.jaxa.jp/gpr/information/product

5.3. Operation of GPM satellite maneuver

NASA has carried out several maneuver operations such as a delta-V maneuver and a Yaw maneuver. In addition, pitch offset maneuvers have also been conducted to check the GPM satellite status. The orbits in which these operations were performed are shown Appendix-A and operation status in the following site. https://gportal.jaxa.jp/gpr/information/product

5.4. Test operation for adjusting the phase code in the KuPR instrument

The JAXA DPR project team has conducted several test operations using different phase codes in the phase shifters in order to mitigate the effects of sidelobe clutter in KuPR. Please be cautious of the periods in these test operations. The orbits in which these operations were performed are shown Appendix-A and operation status in the following site.
https://gportal.jaxa.jp/gpr/information/product

＜Appendix A: Major DPR events＞

Major DPR events until September 2, 2014 are as follows. After September 2, you can visit the following web site to check the DPR status.

https://gportal.jaxa.jp/gpr/information/product

Orbit No.	UTC	DPR Event
#144	2014/3/8 21:54	DPR observation start
#171	2014/3/10 16:29	Change DPR FCIF-B to A
#201	2014/3/12 14:24	GPM Delta-V Maneuver
#206	2014/3/12 22:43	DPR power OFF
#207-231	2014/3/13-14	GPM EEPROM change
#232	2014/3/14 14:14	DPR SCDP-A ON
#232	2014/3/14 14:41	DPR check out restart
#236	2014/3/14 20:02	DPR observation restart
#263	2014/3/16 14:08	Change DPR FCIF-A to B
	2014/3/16 14:59	DPR transmitters off (f1/f2 off) test
#264	2014/3/16 15:49	
#279	2014/3/17 15:10	GPM 180deg Yaw Maneuver (+X to -X)
#294	2014/3/18 13:20	Proper phase code upload
#296	2014/3/18 17:18	DPR SCDP-B ON Observation mode
#310	2014/3/19 14:21	GPM Delta-V Maneuver
#325	2014/3/20 13:41	DPR patch adaption
#328	2014/3/20 17:56	DPR observation restart
#374	2014/3/23 17:26	DPR transmitters off observation
#375	2014/3/23 19:05	
	2014/3/23 19:06	SSPA LNA analysis mode
#377	2014/3/23 22:35	DPR observation restart
#380	2014/3/24 2:11	DPR External calibration
#404	2014/3/25 15:07	DPR transmitters off observation
#418	2014/3/26 12:32	
#419	2014/3/26 14:20	GPM Delta-V Maneuver
#478	2014/3/30 9:53	DPR External calibration
#503	2014/4/1 0:00	DPR External calibration (Yaw + pitch)
#531	2014/4/2 19:47	GPM Delta-V Maneuver
#601	2014/4/7 7:37	DPR External calibration

Orbit No.	UTC	DPR Event
#621	2014/4/8 14:10	Upload new test phase code of KuPR (#1)
#626	2014/4/8 21:46	DPR External calibration (Yaw + pitch)
#647	2014/4/10 6:36	DPR External calibration
#672	2014/4/11 20:43	DPR External calibration (Yaw + pitch)
#675	2014/4/12 1:45	GPM Delta-V Maneuver
#715	2014/4/14 15:28	Upload new test phase code of KuPR (#2)
#731	2014/4/15 15:44	Return to phase code (#1)
#675	2014/4/12 1:45	GPM Delta-V Maneuver
#747	2014/4/16 17:04	GPM Delta-V Maneuver
#748	2014/4/16 17:39	DPR transmitters off observation
#763	2014/4/17 17:07	
#770	2014/4/18 4:22	DPR External calibration (Yaw + pitch)
#795	2014/4/19 18:31	DPR External calibration (Yaw + pitch)
#795	2014/4/19 18:55	Ku/Ka RX ATT change 6dB to 9dB
#810	2014/4/20 17:59	Ku/Ka RX ATT change 9dB to 12dB
#824	2014/4/21 15:36	Ku/Ka RX ATT change 12dB to 6dB
#827	2014/4/21 20:34	GPM Delta-V Maneuver
#885	2014/4/25 13:05	GPM ST alignment and IRUCAL table updates
#886	2014/4/25 14:30	GPM +10 deg. roll slew
	2014/4/25 15:20	GPM +10 deg. pitch slew
#887	2014/4/25 16:10	GPM +10 deg. yaw slew
#901	2014/4/26 13:30	GPM 180deg Yaw Maneuver (-X to +X)
#907	2014/4/27 0:00	GPM -1 deg. pitch slew
#913	2014/4/27 8:20	GPM -1 deg. pitch slew (-2 deg. total)
#918	2014/4/27 16:20	GPM -2 deg. pitch slew (-4 deg. total)
#923	2014/4/28 0:25	
#924	2014/4/28 1:10	Ku/Ka RX ATT change 6dB to 9dB
#933	2014/4/28 15:04	Upload new test phase code of KuPR(#3)
#935	2014/4/28 18:13	Return to phase code(#1)
#964	2014/4/30 15:50	GPM Delta-V Maneuver
#994	2014/5/2 13:20	Upload new test phase code of KuPR (#4)
	2014/5/2 13:21	Ku/Ka RX ATT change 9dB to 6dB
#996	2014/5/2 16:36	Upload new test phase code of KuPR(#5)
#998	2014/5/2 19:44	Ku/Ka RX ATT change 6dB to 9dB

Orbit No.	UTC	DPR Event
	2014/5/2 19:45	Return to phase code (#1)
#1059	2014/5/6 17:35	GPS both A and B ON
#1103	2014/5/14 13:44	
#1073	2014/5/7 15:57	GPM Delta-V Maneuver
#1088	2014/5/8 14:15	Ku SSPA analysis mode (5min)
	2014/5/8 15:08	Ka SSPA analysis mode (5min)
#1089	2014/5/8 15:48	Ku LNA analysis mode (5min)
	2014/5/8 16:44	Ka LNA analysis mode (5min)
#1090	2014/5/8 17:23	Upload new test phase code of KuPR (#6)
#1092	2014/5/8 20:21	Ka SSPA analysis mode (5min)
	2014/5/8 21:12	Upload new test phase code of KuPR (#7)
#1094	2014/5/9 0:16	Return to phase code(#1)
#1150	2014/5/12 14:58	Ku/Ka RX ATT change 9dB to 12dB
#1182	2014/5/14 16:07	GPM Delta-V Maneuver
#1274	2014/5/20 13:30	GMI Deep Space Calibration
#1277	2014/5/20 18:44	
#1288	2014/5/21 11:30	Upload new test phase code of KuPR (#8)
#1290	2014/5/21 14:43	Upload new test phase code of KuPR (#9)
#1292	2014/5/21 17:59	Upload new test phase code of KuPR (#10)
#1294	2014/5/21 21:07	Upload new test phase code of KuPR (#11)
#1296	2014/5/22 0:16	Return to phase code(#1)
#1319	2014/5/23 11:38	Upload new test phase code of KuPR (#12)
#1322	2014/5/23 15:03	Upload new test phase code of KuPR (#13)
#1324	2014/5/23 15:03	Upload new test phase code of KuPR (#14)
#1326	2014/5/23 21:37	Upload new test phase code of KuPR (#15)
#1328	2014/5/24 0:57	Return to phase code(#1)
#1351	2014/5/25 11:44	Change DPR FCIF-B to A (For External Cal.)
		Ku/Ka RX ATT change 12dB to 6dB
#1354	2014/5/25 17:18	DPR External calibration (Yaw + pitch)
#1355	2014/5/25 17:54	Change DPR FCIF-A to B
		Ku/Ka RX ATT change 6dB to 12dB
#1414	2014/5/29 13:59	GPM Delta-V Maneuver
#1430	2014/5/30 13:50	Upload new test phase code of KuPR (#16)
#1431	2014/5/30 15:26	Upload new test phase code of KuPR (#17)

Orbit No.	UTC	DPR Event
#1432	2014/5/30 17:01	Upload new test phase code of KuPR (#18)
#1433	2014/5/30 18:34	Upload new test phase code of KuPR (#19)
#1434	2014/5/30 20:07	Return to phase code(#1)
#1447	2014/5/31 16:06	Upload new test phase code of KuPR (#20)
#1448	2014/5/31 17:53	Upload new test phase code of KuPR (#21)
#1449	2014/5/31 19:59	Return to phase code(#1)
#1477	2014/6/2 15:06	DPR External calibration
#1502	2014/6/4 5:15	DPR External calibration
#1508	2014/6/4 14:13	Upload new test phase code of KuPR (#22)
#1508	2014/6/4 14:56	Upload new test phase code of KuPR (#23)
#1509	2014/6/4 16:39	Upload new test phase code of KuPR (#22)
#1511	2014/6/4 18:59	Return to phase code(#1)
#1539	2014/6/6 14:09	Upload new test phase code of KuPR (#22)
#1541	2014/6/6 17:26	Return to phase code(#1)
#1600	2014/6/4 5:15	DPR External calibration
#1603	2014/6/10 17:38	GPM 180deg Yaw Maneuver (+X to -X)
#1625	2014/6/12 2:58	DPR External calibration
#1646	2014/6/13 11:46	DPR External calibration
#1648	2014/6/13 14:08	Upload new test phase code of KuPR (#24)
#1649	2014/6/13 15:45	Upload new test phase code of KuPR (#25)
#1650	2014/6/13 17:36	Upload new test phase code of KuPR (#26)
#1651	2014/6/13 19:12	Upload new test phase code of KuPR (#27)
#1652	2014/6/13 20:54	Upload new test phase code of KuPR (#28)
#1653	2014/6/13 22:33	Upload new test phase code of KuPR (#29)
#1654	2014/6/14 0:21	Upload new test phase code of KuPR (#30)
#1655	2014/6/14 1:39	Return to phase code(#1)
#1726	2014/6/18 15:17	GPM Delta-V Maneuver
#1769	2014/6/21 9:33	DPR External calibration
#1794	2014/6/22 23:42	DPR External calibration (Yaw + pitch)
#1892	2014/6/29 7:18	DPR External calibration
#1917	2014/6/30 21:27	DPR External calibration
#1942	2014/7/2 12:42	Upload new test phase code of KuPR (#31)
#1944	2014/7/2 14:38	Upload new test phase code of KuPR (#32)
#1945	2014/7/2 16:30	Return to phase code(#1)

Orbit No.	UTC	DPR Event
#1975	2014/7/4 15:07	Upload new test phase code of KuPR (#33)
#1976	2014/7/4 16:44	Upload new test phase code of KuPR (#34)
#1977	2014/7/4 18:24	Return to phase code(#1)
#2015	2014/7/7 5:01	DPR External calibration
#2040	2014/7/8 19:08	DPR External calibration (Yaw + pitch)
#2053	2014/7/9 16:17	GPM Delta-V Maneuver
#2163	2014/7/16 16:32	GPM 180deg Yaw Maneuver (-X to +X)
#2176	2014/7/17 13:22	Upload new test phase code of KuPR (#35)
#2177	2014/7/17 15:03	Upload new test phase code of KuPR (#36)
#2178	2014/7/17 16:37	Upload new test phase code of KuPR (#37)
#2180	2014/7/17 18:47	Return to phase code(#1)
#2184	2014/7/18 1:42	DPR External calibration
#2209	2014/7/19 15:51	DPR External calibration
#2286	2014/7/24 14:54	Change Ku timing delay
#2289	2014/7/24 19:11	Upload new test phase code of KuPR (#38)
#2290	2014/7/24 20:49	Return to phase code(#1)
#2304	2014/7/25 18:07	Upload new test phase code of KuPR (#39)
#2307	2014/7/25 23:26	DPR External calibration
#2332	2014/7/27 13:34	DPR External calibration
#2380	2014/7/30 16:04	GPM Delta-V Maneuver
#2430	2014/8/2 21:12	DPR External calibration (Yaw + pitch)
#2455	2014/8/4 11:21	DPR External calibration
#2455	2014/8/6 20:48	Upload new phase code of KaPR
#2599	2014/8/13 17:55	DPR External calibration
#2624	2014/8/15 8:03	DPR External calibration
#2706	2014/8/20 15:09	GPM Delta-V Maneuver
#2722	2014/8/21 15:40	DPR External calibration
#2747	2014/8/23 5:48	DPR External calibration
#2782	2014/8/25 12:15	Change DPR FCIF-B to A
#2782	2014/8/25 12:30	Upload new test phase code of KuPR (FCIF-A#1)
#2784	2014/8/25 14:34	Upload new test phase code of KuPR (FCIF-A#2)
#2785	2014/8/25 16:13	Upload new test phase code of KuPR

Orbit No.	UTC	DPR Event
		(FCIF-A#3)
#2786	2014/8/25 17:51	Upload new test phase code of KuPR (FCIF-A#4)
#2787	2014/8/25 19:22	Change DPR FCIF-A to B
#2787	2014/8/25 19:24	Return to phase code(#39)

September 4, 2024

Release Notes for the DPR Level-2 and Level-3 products

<Minor changes in the DPR Level-3 products from Version 07C to Version 07D>

The daily and monthly Level-3 DPR algorithms (3DPR) have been updated to correct an error in the collection of Level-2 precipitation statistics partitioned by local time. This correction is only being made on forward data starting with Sept. 1, 2024. Prior data products contain corrupted information on the number of observations partitioned by local time. The fields impacted are: observationCounts/localTime and precipRatelocalTime/* for all grids and swaths. The issue will corrected for past products during the Version 8 reprocessing.

<Minor changes in the DPR Level-2 products from Version 07B to Version 07C>

The GPM Core Observatory satellite performed orbit boost maneuvers on Nov. 7 and 8, 2023 that raised its altitude from 407km to 442km. Details show at the following link.

https://gpm.nasa.gov/missions/gpm/orbit-boost

The orbits in which this operation was performed are shown operation status in the following link.

https://gportal.jaxa.jp/gpr/information/product

In Version 07C, the sensitivity, the spatial resolution and the swath width in the DPR instrument were changed. See full descriptions by the following link.

https://www.eorc.jaxa.jp/GPM/en/boost.html

The updates of the DPR Level 2 algorithm are shown in detail in the following link.

https://www.eorc.jaxa.jp/GPM/doc/algorithm/GPM_Orbit-boost_DPR-note_20240304A.pdf

<Major changes in the DPR Level-2 from Version 07A to Version 07B>

In Version 07B, a new NOAA/NESDIS autosnow was introduced as the input to the DPR Level-2 algorithm. A comparison of precipitation estimates between old and new versions of the autosnow shows that there were differences in specific cases, but few in number. The monthly surface precipitation rate over areas where the snow cover indexes were changed in V07B was very close to that of V07A with the difference less than 1 %.

September 4, 2024

<Major changes in the DPR Level-2 from Version 06A to Version 07A>

Version 07A is the first standard product to account for the Ka-band Precipitation Radar (KaPR) scan pattern change implemented on May 21, 2018. This change in scan pattern allows for a more accurate precipitation estimation method for dual frequency radar, Ku-band and Ka-band Precipitation radar (KuPR and KaPR), to be applied to the entire observation swath.
On the other hand, this led to significant changes of DPR file specifications for common file structures before and after the scan change, in addition to algorithm evolutions. See full descriptions at the following websites:

https://arthurhou.pps.eosdis.nasa.gov/atbd.html
https://www.eorc.jaxa.jp/GPM/en/archives.html

1. Format change in the product

   In the V06X (experimental product), a new format was implemented including "FS" which is defined as the full swath dual-frequency product with 125 m range resolution. In the V07A, this FS format is applied to data taken both before and after the scan pattern change of the KaPR in May 2018 (Figure 1). Note that the DPR/FS has KuPR single frequency data in the outer swath before the scan pattern change, whereas it has DPR dual frequency data in the outer swath after the scan pattern change.

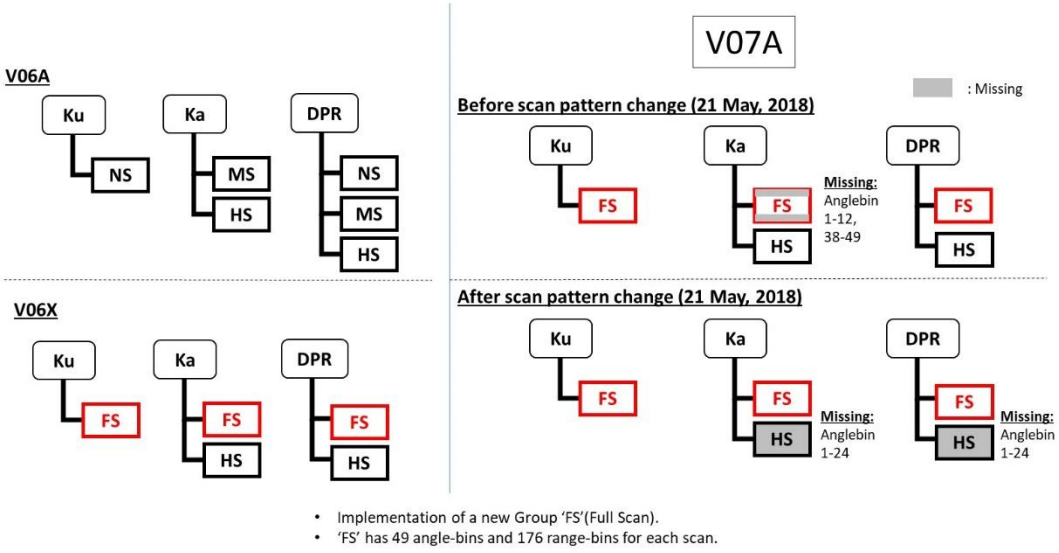

Figure 1. Changes of File structure from V06 to V07

2. In the version 07, the improved sidelobe clutter removal routine was implemented for the single frequency (KuPR, KaPR, and PR) Level-2 algorithms based on the results of Kanemaru et al. (2020, 2021). In addition, a new 3-D precipitation judgement method is implemented to

improve the detectability of precipitation signals. This method uses signals not only in the vertical direction but also the in cross-track and along-track directions. This method is expected to improve the detection of weak, horizontally distributed precipitation that often occurs at high-latitudes. See the ATBD for full descriptions.

3. "flagHail" is newly implemented in the CSF. (Dual frequency only.)
4. The following new items are added to present information about flagHeavyIcePrecip in the CSF: binHeavyIcePrecipTop, binHeavyIcePrecipBottom, and nHeavyIcePrecip.
5. Variables of the Trigger module (TRG) are newly implemented in V07.
6. Changes in the DSD/Solver module from V06 to V07 are listed as follows.
   A) Revision of the relationship between precipitation rate R and volume-weighted mean drop size Dm (the so-called R-Dm relationship). In addition, the parameter ϵ in the R-Dm relationship, which is independent of range in V06, is allowed to vary with range in V07.
   B) Revision of DSD database (used for single-frequency).
   C) Soil moisture effect.

   Note that the soil moisture effect is expected to increase the precipitation amount over land as estimated by the single frequency algorithms by about 14-23%.
7. "precipRateEsurface2" is a surface precipitation estimate based on the *a priori* low-level precipitation profiles (Hirose et al., 2021,). This estimate is stored as an Experimental variable.
8. Other changes in DPR Level-2 algorithm:
   - "binMirrorImageL2" is newly implemented in the Preparation module (PRE) to notify a false precipitation echo that appears at high altitude due to the mirror image.
   - Adjustment factor for KaPR's σ^0 and Z-factor is updated in the Preparation module (PRE).
   - The VER module includes new variables such as the profile of air temperature, a flag that indicates an inversion layer of air temperature, and the rain-free path-integrated attenuation estimate piaNP.
   - Several variable names are changed.
     - zFactorCorrected → zFactorFinal
     - zFactorCorrectedESurface → zFactorFinalESurface
     - zFactorCorrectedNearSurface → zFactorFinalNearSurface
   - Bugs are fixed in several modules. Details of the description for variables are described in Appendix or in the following websites:

     https://www.eorc.jaxa.jp/GPM/en/archives.html

     https://arthurhou.pps.eosdis.nasa.gov/GPMprelimdocs.html

September 4, 2024

CAVEATS for DPR Level-2 V07A:

PRE module

1. In the DPR/FS and KaPR/FS, the following variables have unexpected values only in angle bins 1-12 of the first scan of the granule without any quality indications by the quality flags. This issue occurred only in orbits after the scan pattern change.
   - attenuationNP, piaNP, piaNPrainFree, sigmaZeroNPCorrected, and sigmaZeroCorrected.

CSF module

1. There are bugs on Heavy Ice Precipitation (HIP). The bugs appear only in the data before the antenna scan pattern change (viz., before May 21, 2018). Since the occurrence of HIP is not frequent, the effect of the bugs on the rainfall rate statistics would be small.

   A) flagHeavyIcePrecip in DPR FS does not reflect the Ka-band detection of HIP and the flag value is different from what is designed. The result is based on HIP detected by Ku-band and/or DFRm methods only. Nevertheless, a positive flag value indicates that HIP is detected.

   On the other hand, the additional HIP flags

   binHeavyIcePrecipTop
   binHeavyIcePrecipBottom
   nHeavyIcePrecip

   in the DPR FS structure contain correct values in the inner swath. These flags consist of two dimensional arrays in the DPR FS structure and the second array index distinguishes values obtained by the Ku, Ka, and DFRm methods. In the outer swath, however, binHeavyIcePrecipTop and binHeavyIcePrecipBottom for Ka-band should contain Missing values, but the bugs make them contain values copied from Ku-band. As for the DPR HIP data before May 21, 2018, our suggestion is that users should examine whether flagHeavyIcePrecip > 0 or not. Examination of nHeavyIcePrecip would be a good idea.

   B) In the HS mode data, the additional HIP flags, i.e.,
   binHeavyIcePrecipTop, binHeavyIcePrecipBottom, and nHeavyIcePrecip
   do not contain expected values. The values of those for the Ka-band single frequency HS data are always zero, and those items are even non-existent in the dual frequency DPR HS data structure, the latter of which might be a toolkit bug.

2. A bug on binBBTop: In the V07 DPR FS processing, binBBTop - binBBPeak in the outer swath is bounded by the same parameter value as that in the inner swath. Since the apparent width of BB increases in the outer swath because of the smearing of BB peak, a different parameter value should be used. This bug will be fixed in the next V08. Incidentally, there is not such a bug in the Ku-band single frequency FS processing. The bug was introduced when transplanting the Ku-band FS processing code to the DPR FS processing code. The effect of the bug on the rainfall rate statistics is estimated to be very small.

September 4, 2024

<Major changes in the DPR Level-3 from Version 06A to Version 07A>

1. Format changes in Level-3 DPR Daily/Monthly Products

For a full description of these changes see the Level-3 DPR V07 ATBD document. To accommodate the change in the FS/HS/MS swath structures in the Level-2 products, the Level-3 grids have been restructured as below.

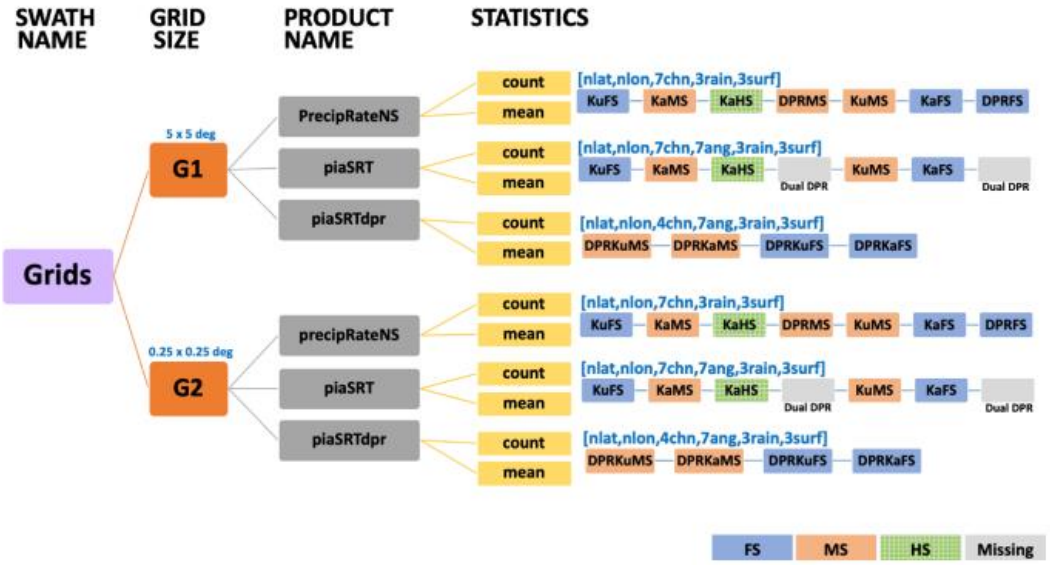

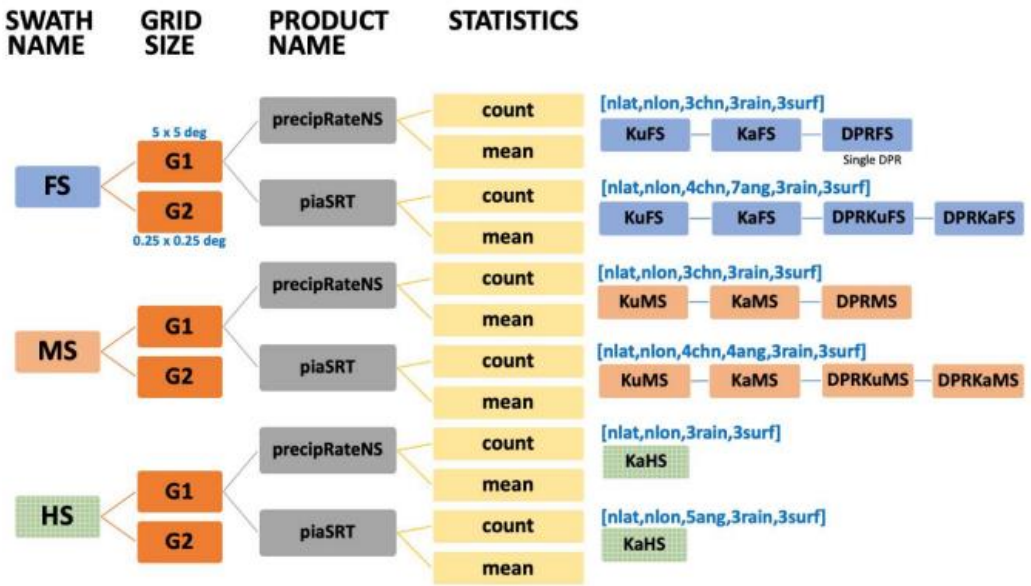

Figure 2. The organization for Level-3 in V06X (upper) and V07A (lower)

CAVEAT for DPR Level-3 V07A:

The Version 07 Level-3 daily products 3DPR-ASC and 3DPR-DES do not accumulate FS statistics (full 49 ifov data) from 5/21/2018 to 5/28/2018 even though the Ka scanning pattern change occurred on 5/21/2018. This will be corrected in a later product version. Users should note that monthly statistics of the Ka and DPR FS/HS data do not cover the entire month of May, 2018.

CAVEAT for DPR Level-3 V06A:

The DPR Daily Product (3DPRD) of Version 06A includes a minor bug. In the array of KuPR channel for ascending path, stratPrecipRateNearSurfMean and stratPrecipRateESurfMean stores convective precipitation (they should have stored stratiform precipitation). This issue is fixed in Version 07A.

September 4, 2024

＜Major changes in the DPR Level-2 from Version 05B to Version 06A＞

1. A new SRT code has been modified to include calculations of Hitschfeld-Bordan PIA as well as a hybrid PIA that combines HB and SRT results. As a result of applying the new PIA in SLV module, erroneously large estimates of high precipitation over ocean (near coast) are mitigated and both DPR (MS) and Ku rain estimates in V06A agree better with Ground Validation data over USA.
2. A new classification algorithm is introduced by the University of Washington (Stacy Brodzik & Robert Houze) to reclassify the stratiform rain type. The new algorithm improved an angle-bin dependence of rain classification and SLH profiles.

Minor changes in DPR Level-2 algorithm:

- Mitigated KaHS's sidelobe clutter and re-calculated the data base for KuPR's sidelobe clutter.
- New variables are introduced. They are flagScanPatten in PRE module, PIAhb, PIAhybrid, reliabFactorHY, reliabFlagHY, stddevEff, stddevHY and zeta in SRT module. For definitions of these variables, the reader is referred to the user manual.
- Modification of surface snow index for the winter temperature inversions.
- Applied the latest SRT data base.
- Bug fix of flagEcho in dual frequency data processing.

September 4, 2024

＜Major changes in the DPR Level-3 products from Version 05B to Version 06A＞

1. New variables are introduced. They are zFactorMeasuredNearSurface, DFRNearSurface, DFRmNearSurface, piaHybrid, piaHybridDPR, piaHB, zeta, and flagHeavyIcePrecip. The definitions of these variables can be found in the user manual.

Figure 3 shows DPR's scan patterns before May 21 2018 (left) and after May 21 2018 (right). KaHS beams scan in the inner swath before May 21 2018, but now they scan in the outer swath and match with KuPR's beams. Numbers in color indicate angle bin numbers for KuPR (blue), KaMS (yellow), and KaHS (red).

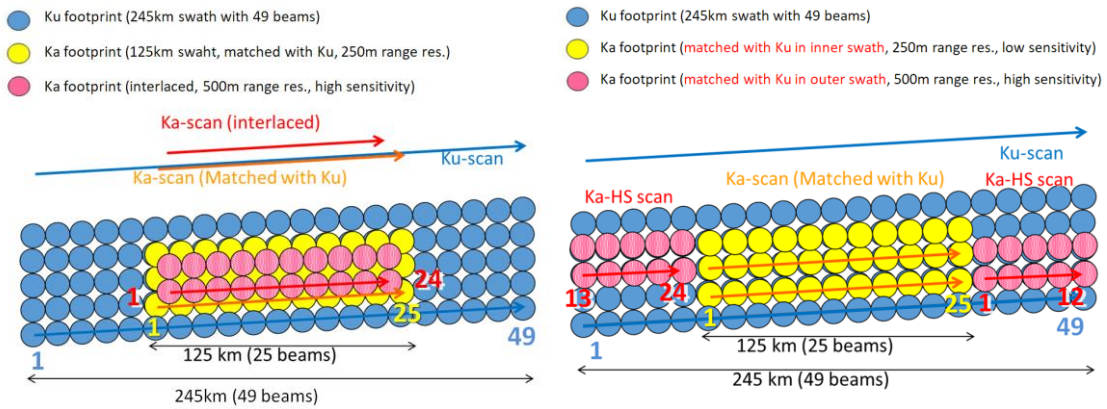

Figure 3. DPR's scan patterns before and after May 21 2018.

1. As of May 21, 2018, the scan pattern of KaHS beams was changed as shown in Figure 3. The KaHS beams scanned in the inner swath before May 21 2018, but now they scan in the outer swath and match with KuPR's beams. Please note that the range resolution of KaHS is 500m and differs from that of the KuPR or KaMS. One scan of KuPR over the full swath consists of 49 beams which are numbered from 1 to 49 in Figure **3** below. The array for one scan of KaMS data consists of 25 beams which correspond to KuPR's central beams from 13 to 37, whereas one scan of KaHS data array for 24 beams consists of two parts. The first 12 elements in the array correspond to KuPR's beams from 38 to 49, and the last 12 elements correspond to KuPR's beams from 1 to 12 of the following scan. All KaMS beams and the first 12 KaHS beams match well with KuPR's beams from 13 to 49. The magnitude of misalignment between these KuPR and KaPR beams is estimated to be less than 50 m after May 21. However, KaHS's beams from 13 to 24 are slightly shifted from the corresponding KuPR beams from 1 to 12 in the along-track direction. The magnitude of misalignment in these beams is about 400 m.

   The dual-frequency algorithm can be applied to the full swath of data after the change of scan pattern. However, because it takes time to develop a new algorithm applicable to the full swath and to adjust the necessary parameters to ensure the quality of the products, KaHS data are not processed in V05B Level-2 algorithm. Missing values are stored in the output variables that use KaHS data. KaHS's received power data are available only in Level-1 products in V05B.

2. All beam directions of KuPR and KaPR were adjusted to match better with the nominal footprint locations. The difference between KuPR and KaPR's footprint centers is now about 30 m at nadir. It was about 300 m before May 21, 2018. This improvement of beam matching is not considered to make a big difference in the Level-2 output products except for very heavy rain cases because the mismatch was small (300 m) from the beginning.

September 4, 2024

＜Major changes in the DPR Level-2 products from Version 04A to Version 05A＞

All users of DPR Level-2 data should keep in mind the following changes in V5 products.

This document describes only the major changes in the Level-2 products. There are some changes in Level-1 that affect the Level-2 products. Please refer to "Release Notes for the DPR Level-1 products" for the details of the changes in Level-1 products.

Among several changes in Level-1 products, the important changes that affect Level-2 products substantially are the following points.

The DPR's system parameters were re-examined. Based on the new calibration results, the offset parameters for the transmitting powers, receiver's gains, the beam widths, and the pulse width of both KuPR and KaPR are redefined. As a result, Zm of KuPR has increased by about +1.3 dB, and Zm of KaPR by about +1.2 dB. The radar surface cross section (σ^0) of KuPR has increased by about +1.2 dB and that of KaPR by about +1.1 dB, although the changes in σ^0 depend slightly on the incidence angle due to the changes in the beam widths. Because of the introduction of the adjustment factors in Level-2 (see below) whose magnitudes vary with time, the numbers mentioned above are not fixed numbers but change with time, especially near the beginning of the GPM mission. In fact, for example, statistics show that an average (over angle) increase in σ^0 at Ku-band is about +1.0 dB, that at KaMS is about +0.6 dB and that at KaHS is about +0.9 dB on the first 5 days in June 2014.

- The FCIF-LUT for the KuPR near the saturation was improved so that the effect of saturation near the saturation level was mitigated.

Changes in Level-2 algorithm:

- In addition to the changes in the DPR Level-1 calibration, adjustment factors are introduced to remove small trends in the overall system gains in KuPR and KaPR. The adjustment factors change the measured received powers only by a small fraction of dB.
- Since the FCIF-LUT for the KuPR near the saturation level was modified to mitigate the effect of saturation, the statistics of σ^0 near the saturation level in the KuPR has changed. This change affects the SRT performance as well. The side-lobe echo cancellation parameters are adjusted to cope with this change as well.
- Measured radar reflectivity factor Zm and surface radar cross section σ^0 are calculated based on the new values of the pulse widths of both KuPR and KaPR. Accordingly, the angle bin dependence of σ^0 has changed slightly.
- A DSD database that depends on the month, region, surface type and rain type was created from the statistics of DSD parameters estimated with the dual-frequency algorithm. The R-

Dm relationship in the DSD database is used as the default R-Dm relationship in the single frequency (Ku-only and Ka-only) data processing before it is modified by other constraints such as the path-integrated attenuation. The introduction of the DSD database has modified the precipitation estimates substantially when they are light (less than about 3mm/h) in many cases. Rain estimates from the Ku-only and dual-frequency algorithms now agree very well.

- New flags are introduced:snowIceCover in the preparation module, flagHeavyIcePrecip and flagAnvil in the classification module, and flagSurfaceSnowfall and surfaceSnowfallIndex in the experimental module. The meanings of these flags should be referred to the user's manual.
- Winter convective storms that give large DFRm (measured Dual-Frequency Ratio) at the storm top are flagged and the corresponding pixels are classified as convective in V5. This category only appears in the inner swath since DFRm is available only there.

Reference

- Hirose, M., S. Shige, T. Kubota, F. A. Furuzawa, H. Minda, H. Masunaga, 2021: Refinement of surface precipitation estimates for the Dual-frequency Precipitation Radar on the GPM Core Observatory using near-nadir measurements. Journal of the Meteorological Society of Japan. Ser. II, 99(5), 1231-1252, https://doi.org/10.2151/jmsj.2021-060
- Kanemaru, K., T. Iguchi, T. Masaki, T. Kubota, 2020: Estimates of Spaceborne Precipitation Radar Pulsewidth and Beamwidth Using Sea Surface Echo Data, IEEE Trans. Geosci. Remote Sens., 58(8), 5291–5303, doi:10.1109/TGRS.2019.2963090
- Kanemaru, K., H. Hanado, K. Nakagawa, 2021: Improvement of the clutter removal method for the spaceborne precipitation radars, the IEEE Geoscience and Remote Sensing Society, the International Geoscience and Remote Sensing Symposium 2021, Virtual Symposium

Release Notes for TRMM/GPM SLH V07

December 2021

Revised in May 2022

For the GPM SLH V07, the LUTs for great mountain ranges in the tropical precipitation regime (rainTypeSLH>200) is newly developed. The areas of the great mountain ranges in the tropical precipitation regime are shown in Figure 1. The separation among the tropics, the great mountain ranges in the tropical precipitation regime, and midlatitudes should be done referring to the rainTypeSLH values stored in the orbital data, and described in Table 1. Note only latent heating is retrieved for great mountain ranges in the tropical precipitation regime in the GPM SLH V07. TRMM SLH V07 algorithm is the same as the GPM SLH V07 algorithm.

The LUT for mid and higher latitudes was newly developed in the GPM SLH V05. In the TRMM/GPM SLH V06A, the same LUT for mid and higher latitudes is applied and LUT for tropics is the same as TRMM SLH V7A. Some recommendations to users of orbital data are listed below, for TRMM/GPM SLH V06A retrieved as tropical precipitation or those as mid latitude precipitation.

Although the SLH algorithm and Tables are the same as GPM SLH V05 for mid-latitude and TRMM SLH V7A for tropics, respectively, because of the change in input PR/KuPR Level 2 data (2APR/2AKu), TRMM/GPM SLH V06A products differ from TRMM SLH V7A and GPM SLH V05 products, respectively.

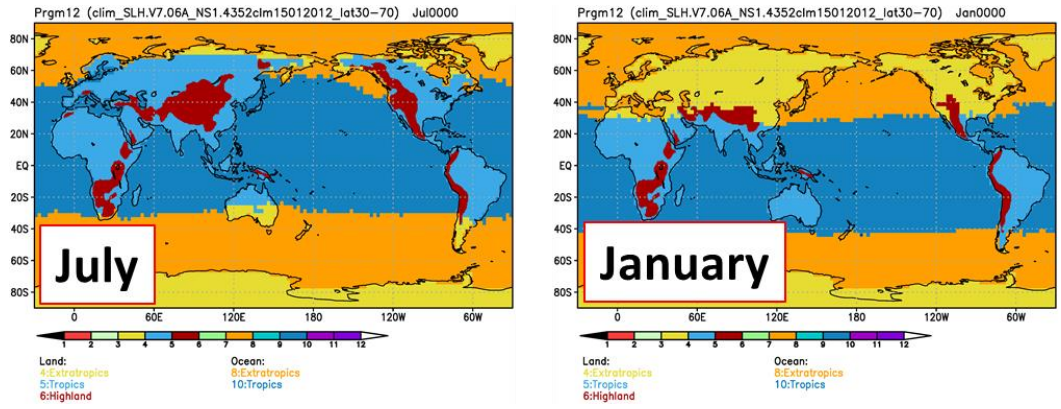

Figure 1 Distribution of the areas (6: Highland) which the LUTs for great mountain ranges in the tropical precipitation regime are applied with the areas (5: Tropics over Land and 10: Tropics over Ocean) where the LUTs for tropics are applied and the areas (4: Extratropics over Land and 8: Extratropics over Ocean) where the LUTs for mid and higher latitudes are applied for July (left) and January (right).

Table 1. Description for rainTypeSLH

(a) Tropics and subtropics	(b) Mid and higher latitudes	(c) Great mountain ranges in the tropical precipitation regime
0: No precipitation	100: No precipitation	200: No precipitation
11: Convective	111: Convective	211: Convective over high-elevation areas 212: Convective over low-elevation areas
21: Shallow stratiform	121: Shallow stratiform	221: Shallow stratiform over high-elevation areas 222: Shallow stratiform over low-elevation areas
31: Deep stratiform 32: Deep stratiform, DI (Intermediary)	131: Deep stratiform, DD, Pmax aloft 132: Deep stratiform, DD, Pmax NS 133: Deep stratiform, DI, Pmax aloft 134: Deep stratiform, DI, Pmax NS 135: Deep stratiform, subzero, Pmax aloft 136: Deep stratiform, subzero, Pmax NS	231: Deep stratiform, DD, Pmax aloft 232: Deep stratiform, DD, Pmax NS 233: Deep stratiform, DI, Pmax aloft 234: Deep stratiform, DI, Pmax NS 235: Deep stratiform, subzero, Pmax aloft 236: Deep stratiform, subzero, Pmax NS
61: Other, Applying table for rainTypeSLH=21	160: Other	261: Other, Applying table for rainTypeSLH=221 262: Other, Applying table for rainTypeSLH=222 263: Other, Applying table for rainTypeSLH=231 264: Other, Applying table for rainTypeSLH=232 265: Other, Applying table for rainTypeSLH=233 266: Other, Applying table for rainTypeSLH=234 267: Other, Applying table for rainTypeSLH=235 268: Other, Applying table for rainTypeSLH=236
Mask		
900: Areas with low melting levels including some mountains except for of great mountain ranges in the tropical precipitation regime 910: Suspicious extreme 920: No precipitation in SLH (precipRate < 0.2 mm/h (0.3 mm/h for tropics) or precipitation depth < 500m) but precipitation exists in 2Aku		

DI: Downward Increasing, DD: Downward Decreasing, NS: Near Surface

It was found that the change of the input KuPR level 2 data from V05 to V06 increased the bias between the KuPR near-surface precipitation and vertically integrated latent heating of SLH V06A. Moreover, some unnatural heating profiles were found associated with precipitation in tropical cyclones. To fix these problems, we revise the algorithm and release the SLH V06B product. Note that the SLH V06B product is available for GPM era since February 2014.

(i) No precipitation or Masked out pixels (rainTypeSLH=0, 100, 200, 300, 900, 910, or 920)

SLH values are not estimated (missing) for raintypeSLH=900 or 910.
SLH values are not estimated (0) for raintypeSLH=0, 100, 200, 300, 920.

(ii) Release note for tropical algorithm (0≦rainTypeSLH <100)

Analysis showed consistency among GPM SLH V04, V05, V06 and TRMM SLH V7A, V07 estimates over the coverage of TRMM/PR during a GPM and TRMM overlapping

observation period (April-June 2014). Note that:

0. Vertical levels are 80 levels.
1. In the V06B SLH, there was a shallow stratiform type (raintypeSLH=21). In V07 SLH this type is no longer used. Heating in all shallow pixels with their precipitation top heights (threshold 0.3mm/hr) lower than the melting level is estimated as convective type (raintypeSLH=11).
2. Differences of sampling between TRMM/PR and GPM/KuPR affect SLH estimates. The greater global coverage of the GPM Core Observatory (65°N/S) compared to the TRMM coverage (35°N/S) decreases sampling of GPM/DPR over the coverage of TRMM/PR, especially at around the satellite inclination latitudes of 35°N/S, affecting SLH estimates there.
3. Retrieval for tropical cyclones and high mountains/winter mid-latitudes pixels will be developed.
4. For tropical latent heating provided in 80 levels, users are recommended to smooth the profile vertical for a few levels to avoid the spurious peak at around 0degC level.
5. The tropical algorithm is sometimes applied at high latitudes in summer. In such cases, pixels to which the tropical algorithm are applied and those to which the mid-latitude algorithm are applied are distributed disorderly. This problem will be fixed in future version.

(iii) Release Note for Mid-latitude algorithm (100≦rainTypeSLH<200)

A. In look up table ranges where sampling numbers did not satisfy the criteria, values are discarded or extrapolated from nearest neighbor bins, depending on the precipitation type. Sampling number criterion is basically 30, but 60 is chosen for deep stratiform LUT with precipitation maximum at the near surface level. Corresponding range for the convective LUT is PTH>11km. Note that in case that a latent heating profile at the candidate bin used for extrapolation has cooling around the middle (or 0.35-0.45) of relative altitudes, for deep stratiform LUT with precipitation maximum at the near surface level, values at the bin are not used for extrapolation and those at its next bin are utilized.

B. Recommendation for horizontal averaging at the utilization of pixel products calculated with the mid-latitude algorithm for SLP or SLG.

B1. Eddy flux convergence in Q1R and Q2 are estimated assuming that the size of "large-scale grids" is 100kmx100km. Therefore, it is recommended to average horizontally in this spatial scale to utilize Q1R or Q2.

B2. Horizontal averaging of about 50km x 50km, or 100 pixels with GPM DPR sampling, is recommended, in order to reduce root mean square errors (RMSE) calculated between estimated LH from LFM-simulated precipitation, to less than a half of the mean value at the LH peak height of ~5.5km (for Case 1).

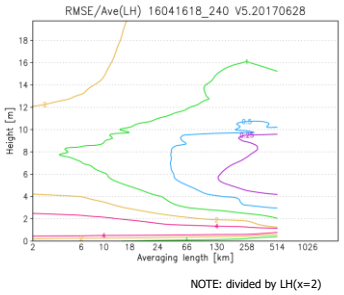

C. CorrectionFactorMidlatType is introduced in the SLH V06B algorithm to consider LH associated with small hydrometeors condensed outside of the precipitating area, transported some distance into the precipitating area, and precipitate. However, the application of this factor in the L2 product is inconsistent in terms of pixel-by-pixel estimation. In the SLH V07 algorithm, this factor is not applied to SLP and SLG products but applied to SLM products. The specific value of the correctionFactorMidlatType is stored in the AlgorithmRuntimeInfo in the L2 product and correctionFactorMidlatType in the L3 product.

(v) Release Note for L3 (gridded; SLG and Monthly; SLM) product

From the TRMM/GPM SLH V06A product, we added the unconditional variables (UnCnd) for all rain type, and modified their variable names to include conditional variables (Cnd). Please refer to the ATBD.

[Note about the missing value for conditional mean]

Note that there are two reasons for missing values for conditional mean (LHCndMean, Q1RCndMean, Q2CndMean), which can be discriminated by 'allPix' values as follows.

1. conditional mean is not defined because there is no precipitation in the grid (precipPix=0), when allPix≠0.
2. missing value is given because the grid value is masked out related to the topography, when and allPix = 0.

[Note about CorrectionFactorMidlatType in SLM]

After the SLH V06B algorithm, heating (LH, Q1R, Q2) has been corrected by the CorrectionFactorMidlatType=0.88 in the area where the midlatitude algorithm is applied. In V07, because this factor is changed to be applied to only the SLM product, but not to the SLP product, the monthly mean of the L2 heating divided by the factor corresponds to the SLM product in the midlatitude area.

November 10, 2023

Release note for GPM Global Rainfall Map (GPM-GSMaP)

The GPM Global Rainfall Map (GPM-GSMaP) Level 3 product version 05A (Algorithm version 8) was released to the public since December 1, 2021, and V05B was released since July 3, 2023. However, because of some reasons, the GPM-GSMaP Level 3 product version 05C was released to the public since November 14, 2023.

Updates from version 05B to version 05C

- Changes of the GMI footprint size due to the orbit boost of the GPM core observatory.

Updates from version 05A to version 05B

- Updated ancillary snow cover and sea ice data inputted into the GSMaP (AUTOSNOW, developed by NOAA/NESDIS).
- Adding NOAA-21 ATMS

Update from version 04 (Algorithm version 7) to version 05A (Algorithm version 8) are following.

A. Passive microwave (PMW) algorithm
    1. Improvement of PMW retrieval technique
        - Adding MHS (Metop-C) and ATMS (Suomi-NPP/ATMS, NOAA-20/ATMS)
        - Update L1 data (TMI, AMSR-E) and decoding tool (AAPP)
        - Retrievals extended to the pole-to-pole (PMW only)
        - Application of dynamic land/ocean classification for all PMW sensors
        - PMW retrieval algorithm considering frozen precipitation depth and static stability in low-level troposphere
        - PMW retrieval for low temperature conditions using scattering signature
        - Implementation of fake precipitation screening due to sea ice, snow etc. over Greenland and Hudson Bay
        - Improvement of snowfall retrievals
        - Improvement of MWS algorithms (Precipitation detection for coastal region etc.)
        - Improvement of rainfall detection method over ocean (implementation of correction method for brightness temperature for rain-free areas)
    2. Improvement of heavy orographic rainfall retrievals considering static stability in low-level troposphere
    3. Update of Database
        - Precipitation profile database (5-year DPR(MS) 06A, algorithm update)
        - Precipitation/no-precipitation classification (5-year KuPR & GMI combined)
        - Surface emissivity (adding TELSEM database outside of PR observation)
        - Change AUTOSNOW format

B. Implementation of Normalization module for PMW retrievals

C. PMW-IR Combined algorithm

   1. Improvement of MVK algorithm
   2. Implementation of histogram matching method

D. Gauge-adjustment algorithm

   1. Improvement of the gauge-calibrated method
   2. Mitigation of artificial patterns appeared in V04

E. Data format

   Adding new variables

   3GSMAPH: reliability flag, surface type, and orographic rain flag

   3GSMAPM: orographic rain ratio

F. Others

   Minor bug fix

For details, following URLs can be helpful for your reference.
http://www.eorc.jaxa.jp/GPM/doc/product_info/release_note_gsmapv05-v8_en.pdf

(For the Japanese)
http://www.eorc.jaxa.jp/GPM/doc/product_info/release_note_gsmapv05-v8_ja.pdf

Followings are remarks and known bugs in current version of GPM-GSMaP product to be fixed in future versions.

Remaining problems

A. Retrieval issues

1. The PMW algorithm introduced in the V05 product overestimates the amount of precipitation for heavy precipitation such as typhoons and convective precipitation, and also confirms that weak precipitation is generally difficult to be detected in MWS. Misidentifying snow or sea ice as precipitation signals has been issued in the V04 product, but this issue has not been fully solved in the V05 product; the extension to the polar regions and the introduction of precipitation and snowfall estimation in low temperature regions make false strong precipitation more apparent, especially in the winter hemisphere. Users should be cautious of estimations over the cold surface (in particular, below 273.2 K).
2. The use of static stability in low-level troposphere as a condition for determining topographic precipitation has made it possible to identify orographic heavy precipitation in inland areas and areas where convective precipitation is dominant. However, overestimation and false-positive of orographic rainfall remain. We examine to resolve this issue.
3. The MMN module introduced in the V05 product largely affects the accuracy after precipitation correction due to the amount and bias of sampling of each sensor. For example, if there is a missing period and the number of missed rainfall cases is large, the average rainfall is likely to deviate from the true value, resulting in an incorrect

value. In addition, the MMN algorithm is not able to change no rainfall to rainfall presence. Improvements in rain/no-rain classification method and the brightness temperature correction method are required.

4. The precipitation estimation of gauge-calibrated hourly rainfall product (GSMaP_Gauge) depends on a large part on the Climate Prediction Center (CPC) Unified Gauge-Based Analysis of Global Daily Precipitation data sets provided by NOAA. If the CPC data sets have good estimation of precipitation in a region, the GSMaP_Gauge data sets also will show good scores in the region. However, in case the CPC data sets under or overestimate the rain fall rate seriously or miss the rainfall event, the GSMaP_Gauge product also estimates or misses the precipitation in a similar manner as the CPC data sets. Note that the CPC data sets and hence the GSMaP_Gauge data do not always show accurate estimation particularly over less dense gauge region.
5. Although the GSMaP_Gauge_NRT is a near real time version of the GSMaP_Gauge, the products do not use the gauge measurement directly. Since the global gauge measurement takes much time to collect and process the data from all over the world, the gauge data is not available in near real time. Hence, in the GSMaP_Gauge_NRT product, only the error parameters derived from the GSMaP_Gauge are used to adjust the GSMaP_NRT estimation, which is named as the GSMaP_Gague_NRT. We would like to know evaluation and validation results of this product for improvement. We appreciate if you give us some feedback.

B. Calibration issues

6. Brightness temperatures used in rainfall retrievals of GCOM-W/AMSR2 and GPM-Core/GMI are bias-corrected using parameters provided by JAXA. These parameters may be modified in future when calibration of each Level 1B data is updated.

November 8, 2023.

Release note for GPM Global Rainfall Map (GPM-GSMaP)

The GPM Global Rainfall Map (GPM-GSMaP) Level 3 product version 04A (Algorithm version 7) was released to the public since January 17, 2017, V04B was released since March 2, 2017, V04C was released since March 27, 2017, V04D was released since May 9, 2017, V04E was released since October 11, 2017, V04F was released since May 11, 2018, V04G was released since May 15, 2019, 04H was released since March 30, 2022, and 04I was released since July 3, 2023. However, because of some reasons, the GPM-GSMaP Level 3 product version 04J was released to the public since November 14, 2023.

Updates from version 04I to version 04J

- Changes of the GMI footprint size due to the orbit boost of the GPM core observatory.

Updates from version 04H to version 04I

- Updated ancillary snow cover and sea ice data inputted into the GSMaP (AUTOSNOW, developed by NOAA/NESDIS).
- Adding NOAA-21 ATMS

Updates from version 04G to version 04H

- Changes of AUTOSNOW format (code update only (i.e. no difference in quality with 04G).

Updates from version 04F to version 04G

- Fix in initialization bugs in the passive microwave radiometer algorithm.
- Changes of the processing environments (OS, intel compiler versions).

Updates from version 04E to version 04F

- Fix in the orographic/nonorographic rainfall classification scheme. Note that this will be effective over the land in latitudes of 20S-60S.
- Improvement in screening of surface snow over the land which may lead to abnormal precipitation.
- Improvement of the gauge-calibrated method in the near-real-time product

Updates from version 04D to version 04E

- Improvement in handling abnormal IR values in the GSMaP_MVK algorithm
- Fix of a very minor issue of the GSMaP_GMI algorithm

Updates from version 04C to version 04D

- Install of a table related to the Tb calibration of GMI L1 V05

Updates from version 04B to version 04C, connected with bug-fixing of "PrecipRateGC" in the following products.

- All standard products in V04A
- Standard products since March 1, 2017 in V04B.

Updates from version 04A to version 04B are following.

- Adding a missing value in "snowProbability" of the GSMaP Hourly (3GSMAPH).
- Bug-fixing in "snowProbability" of the GSMaP Monthly (3GSMAPM).
- Bug-fixing in "satelliteInfoFlag".

Update from version 03 (Algorithm version 6) to version 04A (Algorithm version 7) are following.

1) Improvement of the GSMaP algorithm using GPM/DPR observations as its database
2) Implementation of a snowfall estimation method in the GMI & SSMIS data and a screening method using NOAA multisensor snow/ice cover maps in all sensors
3) Improvement of the gauge-correction method in both near-real-time and standard products
4) Improvement of the orographic rain correction method
5) Improvement of a weak rain detection method over the ocean by considering cloud liquid water

For details, following URLs can be helpful for your reference.
http://www.eorc.jaxa.jp/GPM/doc/product_info/release_note_gsmapv04-v7_en.pdf

(For the Japanese)
http://www.eorc.jaxa.jp/GPM/doc/product_info/release_note_gsmapv04-v7_ja.pdf

Followings are remarks and known bugs in current version of GPM-GSMaP product to be fixed in future versions.

Remaining problems

A. Retrieval issues

1. The snowfall estimation method for the GMI & SSMIS data was installed in the V04 product, but it still needs to be validated and improved further. In addition, several biases and/or gaps may be appeared in the mid-latitude ocean, due to changes of the estimation method. In addition, sometimes, surface snow or sea ice may be misidentified as precipitation signal, especially in spring season. Users should be cautious of estimations over the cold surface (in particular, below 273.2 K).
2. The orographic/non-orographic rainfall classification scheme has been implemented in the GSMaP algorithm for passive microwave radiometers (Yamamoto and Shige, 2014). The scheme is switched off for regions (e.g. the Sierra Madre Mountains in the United States and Mexico) where strong lightning activity occurs in the rainfall type database because deep convective systems for the regions are detected from the scheme involved in the orographic rain condition. The scheme improves rainfall estimation over the entire Asian region,

particularly over the Asian region dominating shallow orographic rainfall. However, overestimation and false-positive of orographic rainfall remain. This is because the orographic rainfall conditions have moderate thresholds for global application. We examine to resolve their problems.

3. The precipitation estimation of gauge-calibrated hourly rainfall product (GSMaP_Gauge) depends on a large part on the Climate Prediction Center (CPC) Unified Gauge-Based Analysis of Global Daily Precipitation data sets provided by NOAA. If the CPC data sets have good estimation of precipitation in a region, the GSMaP_Gauge data sets also will show good scores in the region. However, in case the CPC data sets under or overestimate the rain fall rate seriously or miss the rainfall event, the GSMaP_Gauge product also estimates or misses the precipitation in a similar manner as the CPC data sets. Note that the CPC data sets and hence the GSMaP_Gauge data do not always show accurate estimation particularly over less dense gauge region.
4. Although the GSMaP_Gauge_NRT is a near real time version of the GSMaP_Gauge, the products does not use the gauge measurement directly. Since the global gauge measurement takes much time to collect and process the data from all over the world, the gauge data is not available in near real time. Hence, in the GSMaP_Gauge_NRT product, only the error parameters derived from the GSMaP_Gauge are used to adjust the GSMaP_NRT estimation, which is named as the GSMaP_Gague_NRT. We would like to know evaluation and validation results of this product for improvement. We appreciate if you give us some feedback.

B. Calibration issues

5. Brightness temperatures used in rainfall retrievals of GCOM-W/AMSR2 and GPM-Core/GMI are bias-corrected using parameters provided by JAXA. These parameters may be modified in future when calibration of each Level 1B data is updated.
6. Scan errors may be occasionally found in rainfall retrievals of SSMIS (microwave imager/sounder) on board the DMSP-F16, DMSP-F17 and DMSP-F18 satellites. This problem will be corrected in the future version of L1c data.
7. MHS data used in the GSMaP product was changed form Level 1B to Level 1C. The Scattering Index (SI) in the AMSU-A/MHS algorithm is changed at altitude higher than 40 degrees. However, we have not yet fully evaluated the effect. We would like to know evaluation and validation results of the GSMaP AMSU-A/MHS rainfall retrievals. We appreciate if you give us some feedback.

April 12, 2022

Caveats for the COmbined Radar-Radiometer Algorithm (CORRA) Level 2 Products in the GPM/TRMM V07 Public Releases

The GPM COmbined Radar-Radiometer Algorithm (CORRA) L2 V07 product includes precipitation estimates over the full, 245 km Ku radar swath (Ku+GMI inputs, as well as Ku+Ka+GMI inputs after May 21, 2018), and estimates over the narrower, 125 km inner swath (Ku+Ka+GMI inputs before May 21, 2018). The inputs for the GPM CORRA L2 algorithm are derived from DPR L2 and GMI L1C products. In particular, the CORRA L2 algorithm draws upon inputs from the DPR L2 Preparation Module, Classification Module, Surface Reference Technique Module, and the Vertical Structure Module. From GMI L1C, the GPM L2 algorithm inputs the intercalibrated brightness temperature observations. CORRA has also been extended to produce TRMM precipitation products from a combination of precipitation radar (PR) and TRMM microwave imager (TMI) data, using essentially the same estimation method that is applied to GPM. In this case, estimates based on only the Ku+TMI inputs over the Ku radar swath are produced, since no Ka band radar data are available from TRMM.

During the early GPM mission (prior to June 2014) many tests and modifications of the DPR performance were carried out, and these had an impact on not only DPR products but also the GPM CORRA L2 estimates that depend on them. Therefore, GPM CORRA L2 precipitation estimates from the early mission should be used with caution. A listing of the orbits impacted by these tests and modifications can be obtained from the GPM Radar Team.

Mainlobe and sidelobe clutter contamination of DPR reflectivities is reduced using radar beam reshaping and statistical corrections. The combination of these applications reduces clutter successfully over most surfaces, but there are still "exceptional" regions where clutter signatures are still evident. Also, ice-covered land surfaces produce Ku-band radar surface cross-sections at nadir view that sometime exceed the upper limit of the radar receiver range. Estimates of Ku-band path-integrated attenuation from the Surface Reference Technique Module are possibly biased in these regions. Since radar reflectivities and path-integrated attenuations are utilized by the CORRA L2 algorithm, precipitation estimates in these "exceptional" regions should be used with caution.

The current GPM CORRA L2 algorithm uses the Ku-band radar reflectivities from the Preparation Module to detect either liquid- or ice-phase precipitation. The lowest detectable reflectivity for DPR at Ku band is ~13 dBZ, and so light snow or very light rainfall may not be detected and quantified by the algorithm. The TRMM PR radar has a minimum detectable signal of ~18 dBZ, and so even more light snow and rainfall

may not be quantified by TRMM CORRA.

In addition to the impact of input data from DPR L2, there are uncertainties due to the current limitations of the CORRA L2 algorithm's physical models and other assumptions that can also have an impact on precipitation estimates. In particular, the physical models for scattering by ice-phase precipitation particles now feature realistic nonspherical particle geometries, but these particle models are still undergoing development. The scattering models for ice- and mixed-phase precipitation will likely be improved in future product releases. Also, the effects of radar footprint non-uniform beamfilling and multiple scattering of transmitted power are addressed in CORRA L2, but the strategies that have been implemented to handle these effects are not yet generalized and have not been analyzed in detail. Multiple scattering primarily affects Ka-band reflectivities, and it sometimes eliminates Earth surface reflection in regions of strong radar attenuation (although attenuation can sometimes eliminate the surface signal even if multiple scattering effects are small). Footprint non-uniform beamfilling impacts the interpretation of both Ku- and Ka-band radar data. As a consequence, CORRA L2 precipitation estimates associated with intense convection, in particular, will have greater uncertainties. Finally, the assumed *a priori* statistics of precipitation particle size distributions can have an influence on estimated precipitation. As particle size distribution data are collected during the mission, more appropriate assumptions regarding the *a priori* statistics of particle sizes will be specified in the algorithm. At this stage of the mission, however, relatively simple assumptions regarding particle size distributions have been introduced into the algorithm, and so biases in estimated precipitation rates and the associated particle size distributions can occur. The correct diagnosis of particle sizes in CORRA L2 estimates may require more general constraints on particle size distribution parameters, and these constraints are the subject of ongoing studies.

It should also be noted that both precipitation estimates and retrievals of environmental parameters from CORRA L2 have not yet been comprehensively validated using ground observations. Such a validation effort is under way and will continue to expand after the GPM/TRMM V07 release of products. Therefore, it is very important that users of these public release products keep in contact with the Combined Algorithm Team for updates on the validation of precipitation estimates and any reprocessing's of CORRA L2 products.

Preliminary validation of the GPM CORRA L2 V07 product has revealed good consistency between estimated surface precipitation rate and raingauge-calibrated radar. At footprint scale, matches of the GPM CORRA V07 with raingauge-calibrated radar (Multi-Radar Multi-Sensor [MRMS] product) over the continental US/lower Canada and coastal waters during the June – December 2018 period (post HS scan shift) yielded total low biases of 9% for the Ku+Ka+GMI product and 5% for the Ku+GMI product, with correlations to MRMS of about 0.76 for both products. Considering that the lack of DPR sensitivity contributes a low bias of approximately 7% to the total bias, these are respectable results.

Zonal mean precipitation rates agree well with zonal mean precipitation rates from the Global Precipitation Climatology Project (GPCP V3.2) product within the 40°S to 40°N latitude band over ocean backgrounds. Estimated zonal means at higher latitudes are underestimated relative to GPCP, due in part to the limited sensitivity of the DPR radar to light snow and drizzle. Over the October 2018 – December 2019 period, in the 40°S and 40°N latitude band, CORRA Ku+Ka+GMI L2 estimates over ocean are low-biased by 4% relative to GPCP, while Ku+GMI estimates over ocean are low-biased by 1%. For the same time period and latitude band, Ku+Ka+GMI and Ku+GMI CORRA L2 estimates over land are currently low biased by 13% and 9%, respectively, with the greatest biases occurring in warm, moist tropical and subtropical regimes.

Note that relative to V06, V07 CORRA Ku+Ka+GMI estimates in the 40°S and 40°N band have decreased by 2% over ocean, while Ku+GMI estimates have increased by 7%. Over land in the same latitudinal band, both Ku+Ka+GMI and Ku+GMI estimates have increased by 9% relative to V06. These changes are effected by nudging initial guess drop-size parameters closer to values established from climatological relationships, which leads to greater proportions of smaller drops and higher rain rates at the lighter end of the estimated rain spectrum, particularly over land regions, where radar-derived, path-integrated attenuations and microwave brightness temperatures do not supply additional drop-size information with great certainty. The changes are justified by the greater fidelity of mean CORRA estimates with raingauge-calibrated ground radar estimates over the continental US, better agreement of CORRA with GPCP V3.2 overall, and greater consistency of drop-size distribution parameter relationships relative to climatology.

The TRMM CORRA V07 algorithm precipitation rate estimates compare well with the GPM CORRA V07. Based upon a limited sample of crossover data derived from the April – September, 2014 GPM-TRMM overlap period, there is an overall high bias of TRMM estimates relative to GPM of approximately 6% based upon matched GPM and TRMM footprints, with a correlation of 0.73 between GPM and TRMM.

Mitigation of the low biases in CORRA L2 estimates, particularly over land, is a priority of the algorithm developers and is an active area of PMM research. A radiometer-only precipitation estimation method designed to quantify precipitation rates below DPR detection limits is currently under development and will be introduced in V08 production. In addition, an experimental product for statistically estimating precipitation at the Earth's surface within the DPR ground clutter, based on retrieved values of precipitation above the clutter (near-surface estimates), have been produced and output in CORRA V07. Although preliminary, these surface estimates are substantially increased relative to near-surface estimates, particularly in ocean regions where climatologically, precipitation tends to increase from levels above the clutter toward the surface. *It should be emphasized that these surface estimates are currently experimental, and more work will be required to stabilize and refine these estimates. Users are therefore recommended to still use near-surface*

precipitation estimates until a more rigorous and meteorologically specific clutter correction method is implemented.

There could potentially be significant changes in the CORRA L2 rain rate products in the transition from GPM V07 to V08 due to modifications and improvements of the CORRA algorithm. Since the GPM and TRMM algorithms share the same software "core", future changes in CORRA should apply to both GPM and TRMM. Again, users of the GPM/TRMM V07 public release products should keep in contact with the Combined Algorithm Team for information regarding these changes.

GPM/TRMM CORRA L2 V06 to V07 Changes

Several modifications have been made to the GPM CORRA L2 algorithm in the transition from V06 to V07. These changes can be categorized as changes in algorithm function and changes in output parameters and format. Regarding algorithm function, the basic algorithm mechanics (i.e., estimation methodology) has not changed, and the same mechanics are applied to both the GPM and TRMM data. The GPM estimation method filters ensembles of DPR Ku reflectivity-consistent precipitation profiles using the DPR Ka reflectivities, path integrated attenuations and attenuated surface radar cross-sections at Ku and Ka bands, and GMI brightness temperatures. The filtered profile ensembles are consistent with all of the observations and their uncertainties, and the mean of the filtered ensemble gives the best estimate of the precipitation profile. The TRMM CORRA algorithm filters PR Ku reflectivity-based precipitation profile estimates using path integrated attenuations and attenuated surface radar cross-sections at Ku band, as well as TMI brightness temperatures.

Probably the most impactful change in CORRA V07 concerns the way in which the precipitation drop-size distribution *a priori* assumptions are applied. In both V06 and V07, the precipitation drop-size distribution is assumed to follow a normalized gamma distribution, and the intercept, N_w, and mass-weighted mean diameter, D_m, are adjusted in CORRA during the estimation process. Initial guess values of N_w are drawn from a lognormal distribution and combined with the Ku reflectivity data to derive a D_m profile using a modified Hitschfeld-Bordan procedure. The D_m values are then used to make a second estimate of the N_w, using an empirical $\log N_w - D_m$ curve. Empirical $\log N_w - D_m$ relationships were previously established by Dolan et al. (2018), Bringi et al. (2021) and others, using disdrometer and microphysics probe observations at various locations over the globe. The initial N_w are nudged toward the empirical N_w, and the nudged values are used to again estimate a revised, initial D_m profile using Hitschfeld-Bordan. This two-step initial guess procedure moves initial N_w values higher for lower D_m (lighter precipitation) and lower for higher D_m (heavier precipitation).

In CORRA V06, the procedure just described was only applied to stratiform precipitation, and there were somewhat different drop-size distribution treatments for ocean and land regions. In CORRA V07, there is (a) no distinction between ocean and land in the initial drop-size distribution adjustment, (b) the empirical curve relating $\log N_w$ and D_m for convective precipitation is shifted to slightly higher $\log N_w$ values relative to stratiform, and (c) the nudging of the initial guess N_w toward the empirical values is done more strongly. The upshot of these changes is that the proportion of smaller drops in the initial guess generally increases for smaller D_m, and this leads to increases in precipitation rates at the lighter end of the precipitation spectrum. For heavier precipitation, drop-size distribution adjustments tend to be more controlled by path integrated attenuations and brightness temperatures, if they are reliable. Overall, however, substantial increases in estimated total precipitation are realized in the mean, especially over land regions. Biases of CORRA V07 relative

to ground validation radar and GPCP over land are reduced, and disparities of Ku+Ka+GMI estimates and Ku+GMI estimates over ocean are lessened. In addition, the ocean vs. land contrast of estimated drop-size distributions is less, and the relationships of estimated logN_w and D_m are closer to empirical relationships.

Introduced in CORRA V07 is a clutter or "blind zone" correction of near-surface (above clutter) estimates to create experimental, estimated-surface precipitation rates. The clutter zone of the DPR is roughly 0.7 km at nadir view, rising to over 2 km at the swath edges. Climatological relationships between the near-surface estimates and "surface" estimates (actually, at about 0.8 km above the Earth's surface), were established using nadir-view CORRA V07 precipitation rate profile estimates for ocean/land and convective/stratiform classes. This work follows similar studies by Hirose and Nakamura (2004), Liu and Zipser (2013), and Hirose et al. (2021), but uses CORRA V07 profiles to establish the vertical structure climatologies. The climatological relationships are used to scale the near-surface precipitation rates to statistically estimate surface precipitation rates when the surface level is within the clutter. Over ocean, where cloud updraft speeds are relatively weak, climatological mean precipitation rate profiles tend to increase from radar bins just above the clutter toward the surface, and so precipitation rates are significantly increased over ocean (8%) relative to near-surface values. Over land, climatological profiles tend to show less variation with height, and smaller increases in surface estimates are realized (3%). *Since the climatological precipitation profiles were established based on a limited number of CORRA-retrieved profiles, this clutter correction is deemed experimental in V07, and users are recommended to still use near-surface precipitation estimates until a more rigorous and meteorologically specific clutter correction method is implemented.*

New output variable names and formats have also been introduced in CORRA V07. In particular, the structure name for the Ku+Ka+GMI estimates are called KuKaGMI, and likewise the structure name for the Ku+GMI estimates is now KuGMI. These replace the NS and MS mode structure names of V06, respectively. Similarly, the structure name for the Ku+TMI estimates is now KuTMI. Also, a new structure called OptEst has been included to hold variables derived from an optimal estimation method that fits non-precipitating variables like temperature, humidity, cloud liquid water, and surface emissivity parameters to the radiometer data. These output variables are currently just placeholders, but they will be used in the future to establish background conditions for radiometer-only estimates of precipitation in regions where radar reflectivities are below the minimum detectable of the DPR. Finally, selected variables that were previously estimated at only specified nodal bins of the radar profiles are now defined at full vertical resolution. These include the N_w and D_m profiles, their initial guesses, as well as the profiles of total hydrometeor water contents and fluxes and the liquid portions of those water contents and fluxes. These changes will make it easier to extract and interpret the profiles from CORRA V07.

References:

Bringi, V., M. Grecu, A. Protat, M. Thurai, and C. Klepp, 2021: Measurements of rainfall rate, drop size distribution, and variability at middle and higher latitudes: application to the Combined DPR-GMI Algorithm *Remote Sens.*, **13**, 2412; https://doi.org/10.3390/rs13122412 .

Dolan, B., B. Fuchs, S. A. Rutledge, E. A. Barnes, and E. J. Thompson, 2018: Primary modes of global drop size distributions. *J. Atmos. Sci.*, **75**, 1453-1476.

Hirose, M., and K. Nakamura, 2004: Spatiotemporal variation of the vertical gradient of rainfall rate observed by the TRMM Precipitation Radar. *J. Climate*, **17**, 3378-3397.

Hirose, M., S. Shige, T. Kubota, F. A. Furuzawa, H. Minda, and H. Masunaga, 2021: Refinement of surface precipitation estimates for the Dual-frequency Precipitation Radar on the GPM Core observatory. *J. Met. Soc. Japan* (early online release) DOI:10.2151/jmsj.2021-060.

Liu, C., and E. J. Zipser, 2013: Why does radar reflectivity tend to increase downward toward the ocean surface, but decrease downward toward the land surface? *J. Geophys. Res.: Atmos.*, **118**, 135-148, doi:10.1029/2012JD018134, 2013.

Release Notes for the CSH V05 Level 3 gridded product (3GCSH)

5 July 2017

Changes from V04:

Major changes from V04 include the retrieval of latent heating (LH) over the entire GPM domain (i.e., 67N to 67S), not just the TRMM domain (i.e., 37N to 37S). However, the other remaining CSH products (i.e., eddy heating, microphysical and eddy moistening, and radiation) are still retrieved only over the TRMM domain.

All products are now retrieved at 80 vertical levels every 250 meters AGL starting at the surface (i.e., 0, 250, 500, etc.).

The retrievals for the Tropics (i.e., TRMM domain) are based upon an updated version of the previous CSH algorithm design (Tao et al. 2010). The algorithm still relies upon look-up-tables (LUTs) of model-simulated heating/moistening profiles generated from the Goddard Cumulus Ensemble Model (or GCE), a CRM, which are stored and mapped to satellite grids according to precipitation characteristics. In V04, the previous TRMM V7 CSH LUTs were used. Those LUTs were designed for 0.5 x 0.5 degree TRMM grids (versus the 0.25 x 0.25 degree GPM grids), so the GPM input data in V04 were pre-smoothed to accommodate the coarser resolution of the LUTs. In V05, the LUTs are generated at the GPM grid resolution (0.25 degrees) and are based on 2D multi-week simulations for 6 ocean (vs 5) and 4 land (vs 2) cases (**see Table 1**) using larger domains (512 vs 256 km) and an improved Goddard 4ICE (Lang et al. 2014; Tao et al. 2016) microphysics scheme that includes hail as well as a rain evaporation correction scheme (vs an improved Goddard 3ICE scheme). In addition to the same rain intensity (36) and stratiform fraction bins (20), the LUTs are further differentiated by two new metrics: mean echo top heights (5 bins: 0-2, 2-4, 4-6, 6-8, and above 8 km) and mean low-level (0-2 km) dBZ gradient (increasing or decreasing towards the surface).

Outside the Tropics (i.e., poleward of 37N and 37S), the LH retrievals are based upon a new cold season/ higher latitude algorithm that maps LH profiles based upon 6 NU-WRF (NASA-Unified Weather Research and Forecasting Model) simulations using the same improved 4ICE scheme for 3 eastern US synoptic snow storms and 3 West Coast atmospheric river events. The LUTs are constructed and mapped using the following domain average quantities: storm top heights (6 bins), freezing level (13 bins), max dBZ level (6 bins), dBZ gradient (2 bins), and composite dBZ intensity (90 bins, every 1 dBZ). As with the Tropics, the radar quantities are mean conditional values over each 0.25 x 0.25 degree GPM grid. A radar (composite) coverage factor is then used to scale the corresponding LUT conditional LH profile to obtain the GPM grid average value.

GCE cases for the Revised Tropical LUTs

LUT cases	Type	Location	Period	Duration
ARM 1997	Land	Southern Great Plains	June-July, 1997	29 days
ARM 2002	Land	Southern Great Plains	May-June, 2002	20 days
MC3E	**Land**	**Southern Great Plains**	**April-May, 2011**	**33 days**
GoAMAZON	**Land**	**Amazon Basin**	**Feb-March, 2014**	**40 days**
GATE	Ocean	Tropical Atlantic	Aug-Sept, 1974	20 days
KWAJEX	Ocean	Marshall Islands	July-Sept, 1999	52 days
SCSMEX	Ocean	South China Sea	May-June, 1998	45 days
TOGA COARE	Ocean	Equatorial West Pacific	November, 1992 - February, 1993	120 days
TWPICE	Ocean	Darwin, Australia	Jan-Feb, 2006	6 **(24) days**
DYNAMO	**Ocean**	**Equatorial Indian Ocean**	**Nov-Dec, 2011**	**31 days**

BOLD indicates new additional cases

Table 1

Caveats:

CSH retrievals are derived from Level 2 products from the Combined Radar-Radiometer Algorithm (CMB). Users are encouraged to check related CMB documentation.

CSH retrievals in the tropical TRMM domain are based upon GCE model simulations that do not include terrain. At higher latitudes, the CSH LUTs are based upon NU-WRF simulations that do include terrain. However, areas with domain heights above 500 m were screened out in the construction of the LUTs. Therefore, CSH retrievals both in the Tropics and at higher latitudes in areas with higher terrain should not be relied upon.

Sample Analyses:

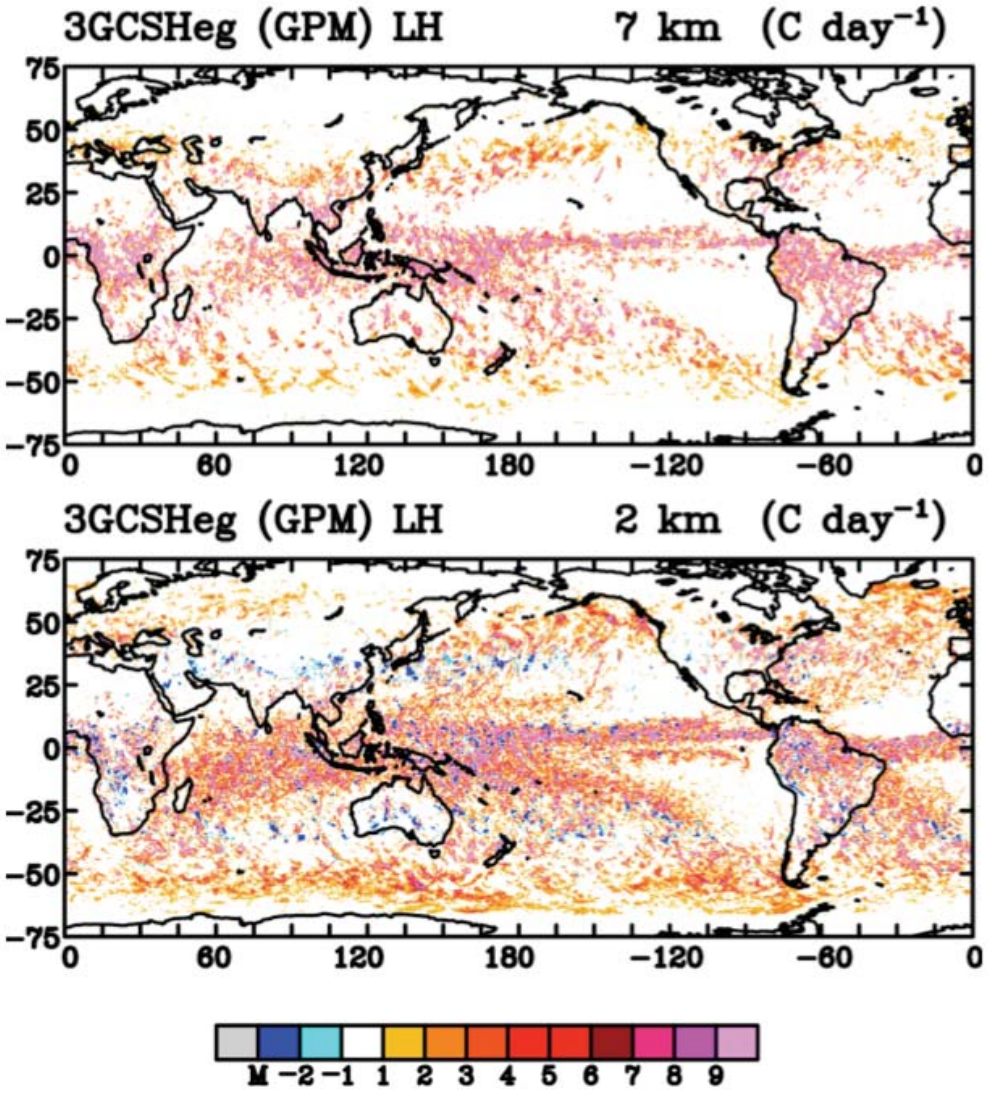

Figure 1. 3GCSH (gridded orbital) V05 LH at 2 and 7 km for April 2014.

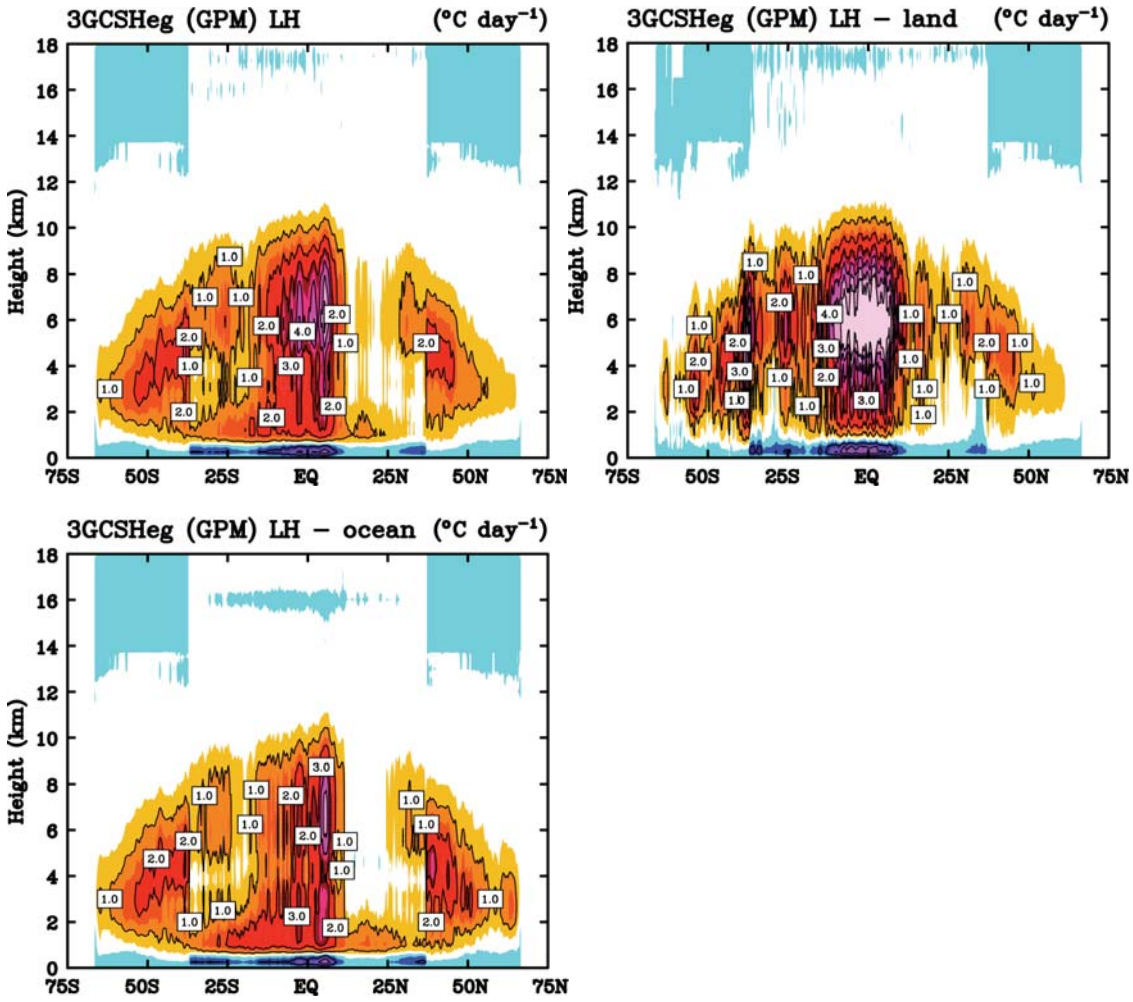

Figure 2. 3GCSH (gridded orbital) V05 zonal average total, land, and ocean LH for April 2014.

References:

Lang, S., W.-K. Tao, J.-D. Chern, D. Wu, and X. Li, 2014: Benefits of a 4th ice class in the simulated radar reflectivities of convective systems using a bulk microphysics scheme. *J. Atmos. Sci.*, **71**, 3583-3612. doi: http://dx.doi.org/10.1175/JAS-D-13-0330.1

Tao, W.-K., S. Lang, X. Zeng, S. Shige, and Y. Takayabu, 2010: Relating convective and stratiform rain to latent heating. *J. Climate.*, **23,** 1874-1893.

Tao, W.-K., D. Wu, S. Lang, J.-D. Chern, C. Peters-Lidard, A. Fridlind, and T. Matsui, 2016: High-resolution NU-WRF simulations of a deep convective-precipitation system during MC3E: Further Improvements and Comparisons between Goddard microphysics schemes and observations. *J. Geophy. Rev. Atmos.*, **121**, 1278-1305, doi:10.1002/2015JD023986.

Release Notes for the CSH V05 Level 3 gridded product (3HCSH)

5 July 2017

Changes from V04:

Major changes from V04 include the retrieval of latent heating (LH) over the entire GPM domain (i.e., 67N to 67S), not just the TRMM domain (i.e., 37N to 37S). However, the other remaining CSH products (i.e., eddy heating, microphysical and eddy moistening, and radiation) are still retrieved only over the TRMM domain.

All products are now retrieved at 80 vertical levels every 250 meters AGL starting at the surface (i.e., 0, 250, 500, etc.).

The retrievals for the Tropics (i.e., TRMM domain) are based upon an updated version of the previous CSH algorithm design (Tao et al. 2010). The algorithm still relies upon look-up-tables (LUTs) of model-simulated heating/moistening profiles generated from the Goddard Cumulus Ensemble Model (or GCE), a CRM, which are stored and mapped to satellite grids according to precipitation characteristics. In V04, the previous TRMM V7 CSH LUTs were used. Those LUTs were designed for 0.5 x 0.5 degree TRMM grids (versus the 0.25 x 0.25 degree GPM grids), so the GPM input data in V04 were pre-smoothed to accommodate the coarser resolution of the LUTs. In V05, the LUTs are generated at the GPM grid resolution (0.25 degrees) and are based on 2D multi-week simulations for 6 ocean (vs 5) and 4 land (vs 2) cases (**see Table 1**) using larger domains (512 vs 256 km) and an improved Goddard 4ICE (Lang et al. 2014; Tao et al. 2016) microphysics scheme that includes hail as well as a rain evaporation correction scheme (vs an improved Goddard 3ICE scheme). In addition to the same rain intensity (36) and stratiform fraction bins (20), the LUTs are further differentiated by two new metrics: mean echo top heights (5 bins: 0-2, 2-4, 4-6, 6-8, and above 8 km) and mean low-level (0-2 km) dBZ gradient (increasing or decreasing towards the surface).

Outside the Tropics (i.e., poleward of 37N and 37S), the LH retrievals are based upon a new cold season/ higher latitude algorithm that maps LH profiles based upon 6 NU-WRF (NASA-Unified Weather Research and Forecasting Model) simulations using the same improved 4ICE scheme for 3 eastern US synoptic snow storms and 3 West Coast atmospheric river events. The LUTs are constructed and mapped using the following domain average quantities: storm top heights (6 bins), freezing level (13 bins), max dBZ level (6 bins), dBZ gradient (2 bins), and composite dBZ intensity (90 bins, every 1 dBZ). As with the Tropics, the radar quantities are mean conditional values over each 0.25 x 0.25 degree GPM grid. A radar (composite) coverage factor is then used to scale the corresponding LUT conditional LH profile to obtain the GPM grid average value.

GCE cases for the Revised Tropical LUTs

LUT cases	Type	Location	Period	Duration
ARM 1997	Land	Southern Great Plains	June-July, 1997	29 days
ARM 2002	Land	Southern Great Plains	May-June, 2002	20 days
MC3E	**Land**	**Southern Great Plains**	**April-May, 2011**	**33 days**
GoAMAZON	**Land**	**Amazon Basin**	**Feb-March, 2014**	**40 days**
GATE	Ocean	Tropical Atlantic	Aug-Sept, 1974	20 days
KWAJEX	Ocean	Marshall Islands	July-Sept, 1999	52 days
SCSMEX	Ocean	South China Sea	May-June, 1998	45 days
TOGA COARE	Ocean	Equatorial West Pacific	November, 1992 - February, 1993	120 days
TWPICE	Ocean	Darwin, Australia	Jan-Feb, 2006	6 **(24) days**
DYNAMO	**Ocean**	**Equatorial Indian Ocean**	**Nov-Dec, 2011**	**31 days**

BOLD indicates new additional cases

Table 1

Caveats:

CSH retrievals are derived from Level 2 products from the Combined Radar-Radiometer Algorithm (CMB). Users are encouraged to check related CMB documentation.

CSH retrievals in the tropical TRMM domain are based upon GCE model simulations that do not include terrain. At higher latitudes, the CSH LUTs are based upon NU-WRF simulations that do include terrain. However, areas with domain heights above 500 m were screened out in the construction of the LUTs. Therefore, CSH retrievals both in the Tropics and at higher latitudes in areas with higher terrain should not be relied upon.

References:

Lang, S., W.-K. Tao, J.-D. Chern, D. Wu, and X. Li, 2014: Benefits of a 4th ice class in the simulated radar reflectivities of convective systems using a bulk microphysics scheme. *J. Atmos. Sci.*, **71**, 3583-3612. doi: http://dx.doi.org/10.1175/JAS-D-13-0330.1

Tao, W.-K., S. Lang, X. Zeng, S. Shige, and Y. Takayabu, 2010: Relating convective and stratiform rain to latent heating. *J. Climate.,* **23,** 1874-1893.

Tao, W.-K., D. Wu, S. Lang, J.-D. Chern, C. Peters-Lidard, A. Fridlind, and T. Matsui, 2016: High-resolution NU-WRF simulations of a deep convective-precipitation system during MC3E: Further Improvements and Comparisons between Goddard microphysics schemes and observations. *J. Geophy. Rev. Atmos.*, **121**, 1278-1305, doi:10.1002/2015JD023986.